August / août 2008 Volume/volume 102 Number/numéro 4 [731]

ANOTHER IMAGE-RICH ISSUE!

Journal

The Journal of the Royal Astronomical Society of Canada

Le Journal de la Société royale d'astronomie du Canada

INSIDE THIS ISSUE

Building for the International Year of Astronomy (IYA2009)

August / août 2008

Journal

Vol. 102, No. 4 Whole Number 731

contents
table des matières

FEATURE ARTICLES / ARTICLES DE FOND

Pixellations II: The Telescope-Camera Connection
p. 145

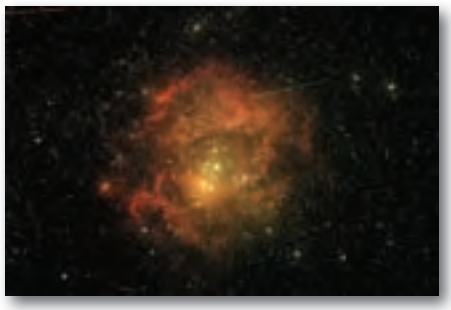

The Chris Graham Robotic Telescope
p. 147

Astrocryptic Answers
p. 158

RASC Dark-Sky Program
p. 150

ROYAL ASTRONOMICAL SOCIETY OF CANADA

SOCIÉTÉ ROYALE D'ASTRONOMIE DU CANADA

DEPARTMENTS

RESEARCH PAPERS/ ARTICLES DE RESEARCH

Cover photo:
A POSSII color-composite image, by Noel Carboni and Daniel Majaess, of the star-forming region designated as the Berkeley 59 / Cepheus OB4 complex. The image is a follow-up to the recent discovery of the primary source illuminating the above complex. The ionizing star was identified by a team of astronomers from Saint Mary's University (Halifax), led by Dr. David Turner (former *Journal* editor) and Dave Lane (current RASC President). Spectroscopic observations from the venerable Dominion Astrophysical Observatory confirmed the discovery, ending a search nearly 50 years in the making.

COLUMNS

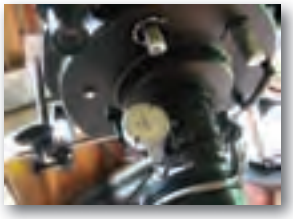

Gizmos
p. 164

Research papers
Articles de researche

Period Changes for the δ Scuti Star YZ Boo

Rachel Ward[1], Paul Delaney[1], Sarah Sadavoy[2], Aaron Maxwell[1], Senthuran Senthilnathan[1], and Sandy Hsu[1]
[1]York University, Toronto, Canada, [2]University of Victoria, Victoria, Canada
Contact: pdelaney@yorku.ca

Abstract: YZ Boo is a high-amplitude δ Scuti star that is one of the stars being monitored by undergraduate students at York University Observatory in Toronto, Canada. Twenty-three new times of maximum light are reported. Along with 149 times from the literature, an updated ephemeris for the star is determined and its O-C plot is presented. Assuming its period is increasing and is changing smoothly, a new value of (1/P)dP/dt is calculated.

Resumé: L'étoile YZ Boo, une de type δ Scuti à grande amplitude, est parmi celles que des étudiants de premier cycle surveillent à l'observatoire de l'université York à Toronto au Canada. Vingt-trois nouvelles périodes de brillance maximale ont été enregistrées. Une éphéméride plus ajour a été établie pour cette étoile à l'aide de 149 périodes additionnelles tirées de la litérature, et le graphique O-C est fourni. En supposant que sa période s'allonge et change en douceur, une nouvelle valeur de (1/P)dP/dt a été calculée.

I. Introduction

High-amplitude δ Scuti (HADS) stars, classified as either Population I or II, are in the process of evolving off the main sequence but within the instability strip for pulsating variables in the Hertzprung-Russell (H-R) diagram (Hog & Petersen 1997). Population I stars have very high metallicity and are found closer to the main sequence than the metal-poor, more highly evolved Population II (SX Phoenicis) stars. HADS are characterized by pulsational periods of several hours (< 0.3 days), amplitudes of variability of 0.3 - 0.7 magnitudes, and low rotational velocities (v sin i < 30 km s^{-1}). While some exhibit multiple modes of pulsation and possibly non-radial modes, many are primarily fundamental-mode pulsators.

In this paper, we are looking at one specific star, YZ Bootis, a Population I variable with fundamental-mode pulsation (Zhou 2002, 2006). Specifically, this paper reports only on the star's period. While other authors have discussed night-to-night light-curve amplitude variations, likely resulting from the contribution of harmonic frequencies of the fundamental, this paper will not add to the discussion. YZ Boo has an apparent magnitude V = 10.57, with a light-curve amplitude of $\Delta V = 0^m.42$ (Zhou 2002, 2006). This star has a relatively long observational history, with photographic observations dating back to 1939 by Tsesevich and photometric observations being

Journal

The *Journal* is a bi-monthly publication of the Royal Astronomical Society of Canada and is devoted to the advancement of astronomy and allied sciences. It contains articles on Canadian astronomers and current activities of the RASC and its Centres, research and review papers by professional and amateur astronomers, and articles of a historical, biographical, or educational nature of general interest to the astronomical community. All contributions are welcome, but the editors reserve the right to edit material prior to publication. Research papers are reviewed prior to publication, and professional astronomers with institutional affiliations are asked to pay publication charges of $100 per page. Such charges are waived for RASC members who do not have access to professional funds as well as for solicited articles. Manuscripts and other submitted material may be in English or French, and should be sent to the Editor-in-Chief.

Editor-in-Chief
Jay Anderson
136 Dupont St
Toronto ON M5R 1V2, Canada
Internet: editor@rasc.ca
Web site: www.rasc.ca
Telephone: (416) 924-7973
Fax: (416) 924-2911

Associate Editor, Research
Douglas Hube
Internet: dhube@phys.ualberta.ca

Associate Editor, General
Michael Attas
Internet: attasm@aecl.ca

Assistant Editors
Michael Allen
Martin Beech
Ralph Chou
Patrick Kelly

Editorial Assistant
Suzanne E. Moreau
Internet: semore@sympatico.ca

Production Manager
James Edgar
Internet: jamesedgar@sasktel.net

Contributing Editors
Martin Beech (News Notes)
Warren Finlay (Deep-Sky Contemplations)
Geoff Gaherty (Through My Eyepiece)
Doug Hube (Deep-Sky Contemplations)
Richard Huziak (Variable Stars)
Bruce McCurdy (Orbital Oddities)
Philip Mozel (A Moment With...)
Guy Nason (Carpe Umbram)
Leslie Sage (Second Light)
Gerry Smerchanski (Gerry's Meanderings)
David Turner (Reviews)
Don Van Akker (Gizmos)

Proofreaders
Ossama El Badawy
Margaret Brons
Angelika Hackett
Terry Leeder
Kim Leitch
Suzanne Moreau
Maureen Okun

Design/Production
Brian G. Segal, Redgull Incorporated

Advertising
James Edgar
Internet: jamesedgar@sasktel.net

Printing
Maritime Digital Colour

The *Journal of The Royal Astronomical Society of Canada* is published at an annual subscription rate of $80.00 by The Royal Astronomical Society of Canada. Membership, which includes the publications (for personal use), is open to anyone interested in astronomy. Applications for subscriptions to the *Journal* or membership in the RASC, and information on how to acquire back issues of the *Journal* can be obtained from:

The Royal Astronomical Society of Canada
136 Dupont St
Toronto ON M5R 1V2, Canada
Internet: nationaloffice@rasc.ca
Web site: www.rasc.ca
Telephone: (416) 924-7973
Fax: (416) 924-2911

Canadian Publications Mail Registration No. 09818
Canada Post: Send address changes to 136 Dupont St, Toronto ON M5R 1V2
Canada Post Publication Agreement No. 40069313

We acknowledge the financial support of the Government of Canada, through the Publications Assistance Program (PAP), toward our mailing costs.

Canada

U.S. POSTMASTER: Send address changes to IMS of NY, PO Box 1518, Champlain NY 12919. U.S. Periodicals Registration Number 010-751.
Periodicals postage paid at Champlain NY and additional mailing offices.
The *Journal* is printed on recycled stock.

recorded by Eggen in 1955 (Szeidl 1981). Its classification has changed from an RR Lyrae to Population I dwarf Cepheid to a more usual classification as a Population I HADS (although the relationship and distinctions between dwarf Cepheids and δ Scuti stars remain topics of discussion in the literature).

Table 1 summarizes various parameters of this star. A compilation of all available times of maximum light for YZ Boo in the literature, Table 3, is supplemented with 23 new times of maximum light obtained at the York University Observatory in Table 5. A slightly improved period and ephemeris for this star are reported. The traditional O-C diagram (observed minus calculated) is also presented. Assuming YZ Boo's period is smoothly changing, based upon the results of the O-C plot, a value for (1/P)dP/dt is calculated.

II. Observations and Data Reductions

A thorough search of the literature was conducted for all available times of maximum light for YZ Boo. Similar searches have been conducted most recently by Zhou (2006) and our Table 2 is comparable to his Table 2. The year of observation, the number of nights observed, the filter(s) used, the number of times of maximum light determined, as well as the source of the data are outlined. Szeidl (1981) and Peniche (1985) represent a very accurate summary and commentary of the earliest data published on YZ Boo. A total of 149 times of maximum light have been collected and are displayed in Table 3.

For completeness, and to reduce confusion for future literature searches, we point out some inconsistencies that exist in the published data record. One data point (HJD 2442900.7073) in Peniche (1985) was incorrectly attributed to Szeidel (1981) and should have been associated with Rolon (1976). Further, it should be noted that from the Heiser and Hardie (1964) paper, the four data points from Heiser and Hardie themselves as well as the six data points attributed to Broglia and Masini that are included in the current analysis are the times of maximum adopted by Szeidl (1981) and Peniche (1985) and subsequent authors. This is different from, for example, the times adopted by Joner (1983) for Heiser and Hardie's data.

Like other studies, the current paper omits the times of maximum light that have been derived from photographic or visual analysis as they are deemed too poorly determined and thus contribute little to the understanding of YZ Boo's behaviour. The seven photometrically determined data points omitted from Zhou's (2006) analysis have also been omitted in this study. These data are displayed in Table 4. With the increasing temporal coverage of the data and the total number of times of maximum light now available, the omission of the data bears little on the final analysis of YZ Boo's behaviour.

In this paper we present a total of 23 new times of maximum light observations for YZ Boo. All data were collected using the York University Observatory's 0.6-m f/13 Cassegrain telescope between 2003 and 2006. The telescope was equipped with an HPC-1 CCD camera manufactured by Spectra Source Instruments during the 2003 observation season. When mounted on the telescope, the HPC-1 CCD camera has a 4.8 by 4.8 arcminute field of view. Since the beginning of the 2005 observation season, the telescope was equipped with an ST-9 CCD camera (Santa Barbara Instrument Group), which has a 5 by 5 arcminute field of view with a focal reducer in the optical path. In order to minimize exposure times and provide better phase coverage, all observations were taken through the *I*-band filter of the Johnson system. Use of this band takes advantage of the red sensitivity of the CCD. Typical exposures were 60 seconds in duration. On all nights, bias, dark and dome flat-field images were obtained for use in pre-processing. *IRAF* was used for the photometric analysis.

For HPC-1 images, corrections were made for DC-offset, two-dimensional bias pattern, dark current, and sensitivity variations using standard techniques (Gilliland 1992). For ST-9 images, similar processing of the images occurred except that there was no correction for bias patterns. Images at the telescope were acquired in such a manner that at least one comparison star was present on all images obtained on any given night. Significant drift of the field over the night caused by tracking error meant not all stars found using DAOPHOT's automatic star finding routines would be on every image. That would have led to a time-consuming extra step of matching the stars afterwards. Since we had only a few stars of interest, we decided to use manual star identification, thereby identifying only the brightest stars that were present on every image taken on a given night. Manual identification proved faster because only the desired stars were identified and measured. Figure 1 has a sample YZ Boo CCD star field and a finder chart. The comparison star GSC 05269-01184 is clearly the star of choice (due to its close spatial proximity and comparable magnitude) for differential photometry with YZ Boo and is used throughout all of our observations.

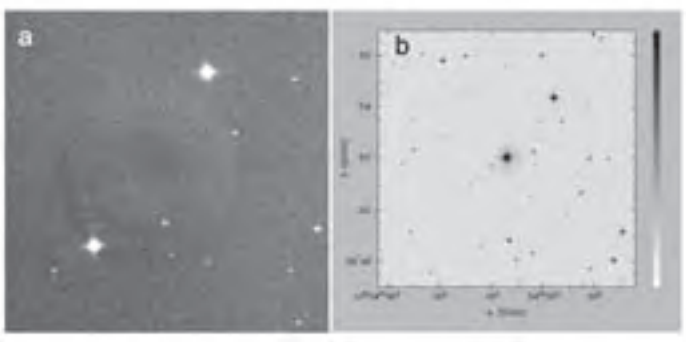

Figure 1 left — A sample image of YZ Boo star field from 2005 July 21 observation with north up and east to the left. YZ Boo is the bright star in the lower left of the image. Right: Finder chart (10' × 10') showing YZ Boo (centered) and comparison star GSC 02569-01184 above and to the right. North up and East to the left.

Differential extinction in the *I*-band between YZ Boo and GSC 05269-01184 for typical observing parameters is much less than our observational uncertainties and so is ignored.

III. Results and discussion

Figure 2 illustrates a light curve observed for YZ Boo on 2005 August 2+3 (UT). The standard deviation in the scatter of the standard comparison star over the duration of the data collection is 0.014 magnitudes. This is quite typical for all of the data collected and reported in this paper. The temporal accuracy for each data point timestamp is less than ± 1 second.

All of the observed times of maximum light (Table 3 and 5 data) were plotted against the Cycle (E) based upon Gieren's (1974) linear ephemeris of

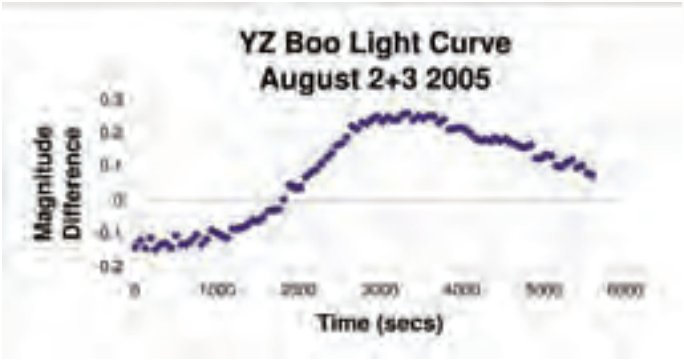

Figure 2 — The above plot is a sample light curve of the differential magnitude between YZ Boo and companion star GSC 02569-01184 from the observation session on 2005 August 2+3.

$$HJD_{max} = 2442146.3546(5) + 0.10409156(1) \times E \quad (1)$$

with the number in parentheses being the uncertainty in the last figure of the preceding coefficient. In this manner, the most accurate period determination (slope of the resulting plot) for YZ Boo was determined to be $0.104091576(3)^d$, marginally longer than the Gieren (1974) period of $0.10409156(1)^d$. The new period results in an improved linear ephemeris of

$$HJD_{max} = 2442146.3552(2) + 0.104091576(3) \times E \quad (2)$$

Table 5 presents the 23 new times of maximum light that we have obtained for YZ Boo. The dates of observations (year, month, day) are in column 1 and the observed times of maximum light, determined by fitting the light curve near the time of maximum light with a high-order polynomial function from the mathematical package Maple, are in column 2. The error in the stated time of maximum light is typically better than $\pm 0.0001^d$ (± 10s). The new ephemeris (2) was used to generate the calculated times of maximum light and the resulting cycle number used is given in column 3, and the differences between

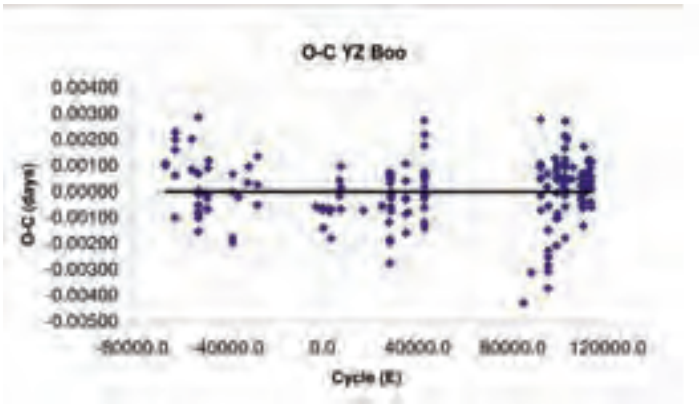

Figure 3 — The O-C diagram of YZ Boo for all 172 data points with a linear trend line drawn.

observed (O) and calculated (C) times of maximum light, O-C, are given in column 4.

Figure 3 is a plot of the O-C differences as a function of cycle number for YZ Boo using all available data. There are 172 data points in total collected over a period in excess of 50 years (1955 to 2007), 23 of the points being new in this paper. It is apparent that significant scatter continues to exist for the available data particularly for recent observations. The standard deviation through the linear least-squares fit to the O-C residuals was = $0^d.00120$.

Considerable discussion continues in the literature (*e.g.* Zhou 2006) as to whether the data can be fit best by a linear or a quadratic ephemeris. If the data are better described by a second-order polynomial, implying that the period of the star is changing smoothly over time, then the quadratic term can yield information about the rate of change of the star's period, as discussed by Breger (1990, 1998) and others. If YZ Boo's mass is constant, then the subtle change in the period of pulsation can be directly linked to the changing radius of the star and evolutionary information about its stellar structure can be inferred.

Figure 4 shows a parabolic fit to the O-C data according to the equation

$$O\text{-}C = 9.32(89) \times 10^{-14} \times E^2 - 5.84(56) \times 10^{-9} \times E + 2.72(30) \times 10^{-4} \quad (3)$$

with a resulting standard deviation = $0^d.00026$, a considerable improvement over the linear fit to the O-C data.

The quadratic coefficient is related to the rate of change of period (Breger 1998) by

$$\text{Coefficient} = 0.5 \times P \times dP/dt \quad (4)$$

The rate of change of period is more usually reported as $(1/P)dP/dt$ with units of $year^{-1}$. (A wide and somewhat confusing range of units and presentations of the changing period of such stars exists in the literature.) Thus for the above quadratic fit, a value for $(1/P)dP/dt = 6.3(6) \times 10^{-9}$ yr^{-1}, comparable to the

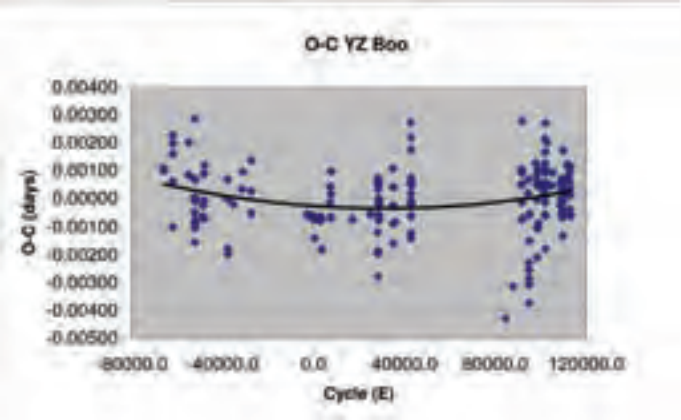

Figure 4 — The O-C diagram of YZ Boo for all 172 data points with a parabolic trend line drawn.

value cited by Zhou (2006) of $5.02(\pm 2.77)\times10^{-9}$ yr^{-1}. This can be compared with the theoretical value (Rodríguez 1995) of $(1/P)\,dP/dt = 1.6\times10^{-9}$ yr^{-1}. A period increase is expected from stellar evolutionary models for a Population I star such as YZ Boo and the value for the rate of period change found with all currently available data is in reasonable agreement. The evidence that the parabolic fit to the O-C data is better than the linear fit is compelling.

In order to determine with certainty the behaviour of YZ Boo and thus the value (or existence) of the rate of change of period, YZ Boo needs to be regularly observed in the future. It is one of the stars that form an ongoing monitoring program conducted by undergraduate students at the York University Observatory in Toronto, Canada. We recall a note by Peniche *et al.* (1985): "...it is impossible right now to decide if the period is constant or if it is varying, but this will be feasible only if the star is regularly observed during the next 40 years." This is as true today as it was then.

IV. Acknowledgments

The authors wish to thank the Department of Physics and Astronomy York University for their funding and support, Patrick B. Hall and Juan Fabregat Llueca for their consultation and input, and the members of the York University Observatory staff who helped to collect this data: Allan Bayntun, Pooi Yee Chung, Behnam Doulatyari, Vincent Huynh, Kenneth Lam, Matthew Lightman, Sara Mazrouei, Tatiana Ouvarova, Brenden Petracek, Olga Pukhovich, Brenda Shaw, and Mark Schuster.

V. References

Agerer, F., Hubscher, J. 2000, IBVS, 4912, 1
Agerer, F., Hubscher, J. 2003, IBVS, 5485, 1
Agerer, F., Dahm, M., & Hubscher, J. 1999, IBVS, 4712, 1
Berger, M. 1990, PASP Conf. Ser. 11, 263
Berger, M., Pamyatnykh, A.A. 1998, A&A, 332, 958
Broglia, P., Masani, A. 1957, Mem. Soc. Astr. Italy 28, 1 (Contr. Oss. Astr. MilanoMerate No. 102)
Broglia, P. 1961, Mem. Soc. Astr. Italy 32, 7
Derekas, A. *et al.* 2003, A&A, 402, 733
Eggen, O. 1955, PASP, 67, 354
Fitch, W.S., Wisniewski, W.Z., & Johnson, H.L. 1966, Comm. Lunar and Planetary Lab. 5
Gieren, W., Gieseking, F., & Hoffmann, M. 1974, A&A. 37, 443
Gilliland, R. L. 1992, PASP Conf. Series No. 23, 68
Hamdy, M.A., Mahdy, H.A., & Soliman, M.A. 1986, IBVS, 2963
Heiser, A.M., Hardie, R.H. 1964, ApJ, 140, 694
Hog, E., Petersen, J.O. 1997, A&A, 323, 827
Hubscher, J. 2005, IBVS 5643, 1
Hubscher, J., Paschke, A., & Walter, F. 2006, IBVS 5731, 1
Jin, H., Kim, S.-L., Kwon, S.-G., Youn, J.-H., Lee, C.-U., Lee, D.-J., & Kim, K.-S. 2003, A&A, 404, 621
Jiang, S.-Y. 1985, Acta. Astron. Sinica, 26, 297
Joner, M.D., McNamara, D.H. 1983, PASP, 95, 433
Kim, C., Joner, M.D. 1994, Astrophys. & Space Sci. 218, 113
Klingenberg, G., Dvorak, S.W., & Robertson, C.W. 2006, IBVS 5701, 1
Langford, W.R. 1976, Dissertation, Brigham Young University
Peña, J.H., González, D., Peniche, R. 1999, A&AS, 138, 11
Peniche, R., González, S. F., Peña, J.H. 1985, PASP, 97, 1172
Rodríguez, E., López de Coca, P., Costa, V., & Martin, S. 1995, A&A, 299, 108
Rolon, A.S., Tolman, B.W., & McNamara, D.H. 1976, Private Communication (Peniche to McNamra)
Spinrad, H. 1959, ApJ, 130, 539
Szeidl, B.N., Mahdy, H.A. 1981, Comm. Konkoly Obs. of the Hungarian Academy of Sciences, No. 75
Zhou, A.-Y. 2002, ChJAA, 2, No.1, 43
Zhou, A.-Y. 2006, Astrophys. & Space Sci., 301, 11

Tables 1 - 5 on the following pages...

Spectral Type	A6 - F1
Right Ascension (2000)	$15^h\ 24^m\ 7.0^s$
Declination (2000)	+36° 52′ 0.6″
Fe/H	-0.39
Te (K)	7650
log g	3.84
Q	0.032

Table 1 — Basic data for YZ Boo: Fe/H, T_e, log g and Q from Pena (1999)

Year	Nights	Filter	Maxima	Source
1955	1	(blue)	2	Eggen (1955)
1956	4	blue, yellow	5	Broglia & Masani (1957)
1958	2	blue, yellow	2	Spinrad (1959)
1959 - 1979	15	V	20	Szeidl (1981)
1960	5	Blue	6	Broglia (1961)
1963	4	V	4	Heiser (1964)
1964	1	V	1	Fitch (1966)
1965 - 1966	4	y	5	Langford (1976)
1974	1	V	3	Gieren (1974)
1976	4	y	6	Rolon (1976)
1981 - 1984	4	V	4	Jiang (1985)
1982	5	y	7	Joner (1983)
1982 - 1984	8	V	11	Peniche (1985)
1984	1	V	1	Kim (1994)
1986	13	V	16	Hamdy (1986)
1998	1	None	1	Agerer (1999)
1999	1	None	1	Agerer (2000)
2001	5	V	9	Derekas (2003)
2000 - 2003	9	V	20	Zhou (2006)
2002 - 2003	3	V	3	Agerer (2003)
2002 - 2003	2	V	3	Jin (2003)
2002 - 2006	5	None – V	12	Klingenberg (2006)
2003 - 2004	2	None	2	Hunscher (2005)
2004 - 2005	3	V	5	Hubscher (2006)
Total	103		149	

Table 2 — Literature search summary for 149 times of maximum light reported for YZ Boo

Source	HJD (Observed)	Cycle (E)	O-C (days)
Derekas (2003)	2452025,36950	94907	-0.00489
Broglia (1957)	2435688,40900	-62041	-0.00078
Agerer (1999)	2450950,41640	84580	-0.00428
Agerer (2000)	2451293,39930	87875	-0.00313
Peniche (1985)	2445095,79400	28335	0.00399
Peniche (1985)	2445095,89700	28336	0.00289
Peniche (1985)	2445096,00300	28337	0.00480

Table 4 — All seven published and omitted photometrically determined times of maximum light prior to the current paper.

Observation date	HJD (Observed)	Cycle (E)	O-C (days)
2003-07-30+31	2452851,65532	102845	0.00201
2005-05-30+31	2453522,62789	109291	0.00028
2005-06-01+02	2453523,66924	109301	0.00072
2005-06-02+03	2453524,60482	109310	-0.00053
2005-06-06+07	2453528,66552	109349	0.00060
2005-06-07+08	2453529,60196	109358	0.00022
2005-06-22+23	2453544,59091	109502	-0.00002
2005-06-23+24	2453545,63146	109512	-0.00039
2005-07-07+08	2453559,68356	109647	-0.00065
2005-07-11+12	2453563,63838	109685	-0.00131
2005-07-14+15	2453566,65874	109714	0.00039
2005-07-22+23	2453574,67336	109791	-0.00004
2005-07-27+28	2453579,66969	109839	-0.00010
2005-07-29+30	2453581,64774	109858	0.00021
2005-08-08+09	2453591,64040	109954	0.00008
2005-08-10+11	2453593,61979	109973	0.00173
2006-05-23+24	2453879,66263	112721	0.00092
2006-05-29+30	2453885,59454	112778	-0.00039
2006-06-06+07	2453893,71443	112856	0.00035
2006-06-12+13	2453899,64786	112913	0.00056
2006-06-20+21	2453907,66247	112990	0.00012
2006-07-07+08	2453924,62868	113153	-0.00059
2006-07-13+14	2453930,66774	113211	0.00115

Table 5 — 23 new times of maximum light. O-C values determined use the revised ephemeris, equation (2), for the "calculated" (C) time of maximum light

Source	HJD (Observed)	Cycle (E)	O-C (days)		Source	HJD (Observed)	Cycle (E)	O-C (days
Eggen (1955)	2435282,76600	-65938	0.00109		Fitch (1966)	2438466,92600	-35348	-0.00021
Eggen (1955)	2435282,87000	-65937	0.00100		Langford (1976)	2438878,92100	-31390	0.00034
Broglia (1957)	2435689,44970	-62031	-0.00099		Langford (1976)	2438908,90000	-31102	0.00096
Broglia (1957)	2435695,38620	-61974	0.00229		Langford (1976)	2439295,91100	-27384	-0.00051
Broglia (1957)	2435695,49000	-61973	0.00199		Langford (1976)	2439301,74200	-27328	0.00136
Broglia (1957)	2435698,40320	-61945	0.00063		Langford (1976)	2439301,84500	-27327	0.00027
Broglia (1957)	2435699,34100	-61936	0.00161		Gieren (1974)	2442146,45860	1	-0.00071
Spinrad (1959)	2436428,81400	-54928	0.00084		Gieren (1974)	2442146,56270	2	-0.00070
Spinrad (1959)	2436429,75200	-54919	0.00202		Gieren (1974)	2442146,35460	0	-0.00062
Szeidl (1981)	2436709,55100	-52231	0.00287		Rolon (1976)	2442900,70730	7247	0.00043
Szeidl (1981)	2436712,46340	-52203	0.00070		Rolon (1976)	2442900,81080	7248	-0.00016
Szeidl (1981)	2436713,39850	-52194	-0.00102		Rolon (1976)	2442948,90060	7710	-0.00067
Szeidl (1981)	2436713,50310	-52193	-0.00051		Rolon (1976)	2442952,85690	7748	0.00015
Szeidl (1981)	2436714,43890	-52184	-0.00154		Rolon (1976)	2442956,70830	7785	0.00016
Szeidl (1981)	2436716,41740	-52165	-0.00078		Rolon (1976)	2442956,81320	7786	0.00097
Szeidl (1981)	2436716,52220	-52164	-0.00007		Jiang (1985)	2444753,12000	25043	-0.00055
Szeidl (1981)	2436717,35450	-52156	-0.00050		Jiang (1985)	2445794,24490	35045	0.00041
Szeidl (1981)	2436723,49630	-52097	-0.00011		Jiang (1985)	2445795,28510	35055	-0.00030
Szeidl (1981)	2436724,43320	-52088	-0.00003		Jiang (1985)	2445796,22330	35064	0.00107
Szeidl (1981)	2436724,53800	-52087	0.00068		Joner (1983)	2445136,90560	28730	-0.00059
Szeidl (1981)	2436725,37010	-52079	0.00005		Joner (1983)	2445137,73890	28738	-0.00002
Szeidl (1981)	2436725,47330	-52078	-0.00085		Joner (1983)	2445137,84370	28739	0.00069
Szeidl (1981)	2442187,47000	395	-0.00139		Joner (1983)	2445147,83630	28835	0.00050
Szeidl (1981)	2442464,56240	3057	-0.00077		Joner (1983)	2445148,77250	28844	-0.00013
Szeidl (1981)	2442464,66660	3058	-0.00066		Joner (1983)	2445149,70870	28853	-0.00075
Szeidl (1981)	2442522,43740	3613	-0.00068		Joner (1983)	2445149,81330	28854	-0.00024
Szeidl (1981)	2442523,47720	3623	-0.00180		Peniche (1985)	2445076,95000	28154	0.00056
Szeidl (1981)	2441860,41510	-2747	-0.00056		Peniche (1985)	2445077,78100	28162	-0.00117
Szeidl (1981)	2443936,62550	17199	-0.00073		Peniche (1985)	2445077,88700	28163	0.00074
Broglia (1961)	2437077,51120	-48696	-0.00065		Peniche (1985)	2445096,82900	28345	-0.00193
Broglia (1961)	2437098,43400	-48495	-0.00026		Peniche (1985)	2445097,87000	28355	-0.00185
Broglia (1961)	2437120,39750	-48284	-0.00008		Peniche (1985)	2445097,97400	28356	-0.00194
Broglia (1961)	2437120,50100	-48283	-0.00068		Peniche (1985)	2445098,80900	28364	0.00033
Broglia (1961)	2437137,36540	-48121	0.00089		Peniche (1985)	2445098,91000	28365	-0.00276
Broglia (1961)	2437168,38500	-47823	0.00120		Peniche (1985)	2445800,90610	35109	-0.00025
Heiser (1964)	2438206,69550	-37848	-0.00177		Peniche (1985)	2445801,94640	35119	-0.00086
Heiser (1964)	2438209,82000	-37818	-0.00001		Peniche (1985)	2445802,98660	35129	-0.00158
Heiser (1964)	2438214,71300	-37771	0.00068		Kim (1994)	2445886,78110	35934	-0.00080
Heiser (1964)	2438221,68450	-37704	-0.00195		Hamdy (1986)	2446606,36970	42847	0.00274
Hamdy (1986)	2446612,30000	42904	-0.00018		Zhou (2006)	2452764,21765	102005	0.00126
Hamdy (1986)	2446612,40400	42905	-0.0002		Zhou (2006)	2452768,06945	102042	0.00167
Hamdy (1986)	2446613,33990	42914	-0.00120		Zhou (2006)	2452768,17195	102043	0.00008
Hamdy (1986)	2446614,27730	42923	-0.00062		Zhou (2006)	2452768,27654	102044	0.00058

Hamdy (1986)	2446614,38250	42924	0.00049		Zhou (2006)	2452777,12196	102129	-0.00178
Hamdy (1986)	2446615,31930	42933	0.00046		Zhou (2006)	2452777,23055	102130	0.00271
Hamdy (1986)	2446617,29720	42952	0.00062		Agerer (1999)	2450950,41640	84580	-0.00428
Hamdy (1986)	2446618,33610	42962	-0.00139		Agerer (2000)	2451293,39930	87875	-0.00313
Hamdy (1986)	2446619,27450	42971	0.00018		Agerer (2003)	2452327,55350	97810	0.00127
Hamdy (1986)	2446620,31700	42981	0.00177		Agerer (2003)	2452692,60160	101317	0.00021
Hamdy (1986)	2446621,35690	42991	0.00075		Agerer (2003)	2452763,48760	101998	-0.00015
Hamdy (1986)	2446622,29360	43000	0.00063		Hubscher (2005)	2452737,46540	101748	0.00055
Hamdy (1986)	2446623,33380	43010	-0.00009		Hubscher (2005)	2453105,42950	105283	0.00093
Hamdy (1986)	2446624,27130	43019	0.00059		Hubscher (2006)	2453056,61010	104814	0.00048
Hamdy (1986)	2446624,37700	43020	0.00220		Hubscher (2006)	2453462,46320	108713	0.00052
Derekas (2003)	2451985,61160	94525	0.00020		Hubscher (2006)	2453462,56650	108714	-0.00027
Derekas (2003)	2452001,53810	94678	0.00069		Hubscher (2006)	2453483,38530	108914	0.00022
Derekas (2003)	2452028,39020	94936	-0.00284		Hubscher (2006)	2453483,48910	108915	-0.00008
Derekas (2003)	2452028,49460	94937	-0.00253		Klingenberg (2006)	2452374,70620	98263	0.00049
Derekas (2003)	2452028,59750	94938	-0.00372		Klingenberg (2006)	2452374,81064	98264	0.00084
Derekas (2003)	2452030,36930	94955	-0.00148		Klingenberg (2006)	2452392,71252	98436	-0.00104
Derekas (2003)	2452030,47260	94956	-0.00227		Klingenberg (2006)	2452392,81760	98437	-0.00005
Derekas (2003)	2452030,57590	94957	-0.00306		Klingenberg (2006)	2452392,91966	98438	-0.00208
Derekas (2003)	2452039,32210	95041	-0.00056		Klingenberg (2006)	2452432,68370	98820	-0.00102
Jin (2003)	2452422,06783	98718	0.00045		Klingenberg (2006)	2452432,78942	98821	0.00061
Jin (2003)	2452422,17251	98719	0.00104		Klingenberg (2006)	2453798,47144	111941	0.00116
Jin (2003)	2452761,82265	101982	0.00037		Klingenberg (2006)	2453798,57500	111942	0.00062
Zhou (2006)	2451692,07368	91705	0.00052		Klingenberg (2006)	2453798,67870	111943	0.00023
Zhou (2006)	2451692,17774	91706	0.00049		Klingenberg (2006)	2453800,86516	111964	0.00077
Zhou (2006)	2451692,28233	91707	0.00099		Klingenberg (2006)	2453800,96972	111965	0.00124
Zhou (2006)	2451693,11499	91715	0.00091					
Zhou (2006)	2451693,21923	91716	0.00106					
Zhou (2006)	2451704,25172	91822	-0.00015					
Zhou (2006)	2451705,08739	91830	0.00278					
Zhou (2006)	2451705,18920	91831	0.00050					
Zhou (2006)	2451705,29207	91832	-0.00072					
Zhou (2006)	2452438,20073	98873	-0.00084					
Zhou (2006)	2452763,07353	101994	0.00215					
Zhou (2006)	2452763,17640	101995	0.00093					
Zhou (2006)	2452763,28066	101996	0.00110					
Zhou (2006)	2452764,11172	102004	-0.00058					

Table 3 — All 149 published (and retained) times of maximum light (prior to the current paper). O-C values determined use the revised ephemeris, equation (2) for the "calculated" (C) time of maximum light.

Magnitude Changes in a Suspected Variable Star

by Alaina Edwards, Winnipeg Centre (alaina@edwardsathome.com)

Introduction

As technology advances, it allows us to increase our knowledge of different aspects of the world in which we co-exist. By using newer advances and theories, we have the ability to learn more about what we were once unable to explain. One type of study that has benefited immensely from technology is the wide field of astronomy. A number of mechanisms, such as telescopes and satellites, have been developed to expand the knowledge we have in this field. Telescopes allow the user to better view an object that is at a distance by magnifying it. This is done by increasing the amount of light that reaches our eyes, allowing us to view objects that aren't easily seen at great distances.

One such advancement is the *Hipparcos* satellite that was launched on 1989 August 8. The satellite measured the angle of parallax to determine distances to a large number of stars. It is also responsible for cataloguing suspected variable stars[1]. These are stars that change their brightness, some over a regular period of time, others at irregular intervals. The *Hipparcos* satellite has assisted in cataloguing over 30,000 variable stars and thousands more that are suspected of being variable.

There are two different types of variable stars: intrinsic and extrinsic. Intrinsic variables have light variations caused by physical changes in the star. Intrinsic variable stars are further broken down into two classes: pulsating and eruptive. Pulsating variables show a periodic expansion and contraction of the star's surface. A star experiencing radial pulsations remains spherical in shape, as opposed to a star with non-radial pulsations, which may change from a spherical shape periodically. Eruptive variables, also known as cataclysmic variables, are stars that undergo infrequent extreme outbursts caused by thermonuclear processes in either their surface layers or in the interior of the star.

Extrinsic variable stars result when the star's changes in brightness are caused by a smaller, darker star passing in front of the suspected variable or by structures on the surface of the star itself. These two factors allow extrinsic variable stars to be separated into two classes: eclipsing binaries and rotating stars. Eclipsing binary stars are pairs of stars that have an orbital plane lying near the observer's line-of-sight. The two objects periodically block one another, causing an overall decrease in the brightness in the system. Lastly, rotating stars from the extrinsic class show small changes in light that may be caused by bright or dark spots and patches on their surface. To complicate the picture, rotating stars that show variability are commonly found in binary systems.

Flare stars and irregular variables are two other uncommon types of variable stars. Flare stars are sometimes known as UV Ceti stars. They are intrinsically faint, cool, and red, main-sequence stars that tend to have intense outbursts from specific areas on their surface. The outburst results in an increase in brightness of two or more magnitudes in a few seconds. Afterwards, there is a decrease to the star's normal minimum in about 10 to 20 minutes.

Irregular variables, including most of the Red Giants[2], are pulsating variables that show brightness variation with an irregular periodicity.

Methodology

The purposes and goals of this study are:

1. to observe and record patterns of a suspected variable star, identified by the *Hipparcos* satellite, using a remotely controlled telescope located in Australia;
2. to determine whether or not it is a true variable star;
3. if it proves to be a true variable star, determine what type of variable star it is by studying its variation in brightness over a period of time;
4. to submit collected data and information to the AAVSO International Database.

If a suspected variable star is observed to change in brightness or magnitude[3], it can be concluded to be a true variable star.

Dr. David McKinnon, Associate Professor of Science and Education at Charles Sturt University, residing in Bathurst, Australia, helps students across the world access the stars and other objects in the Solar System and Universe. Through his remote telescope (Figure 1), students can target and observe a wide range of objects. The telescope was built by him and resides in his backyard; he has made the instrument accessible and available to schools around the world through the Internet. Dr. McKinnon also works both alongside and remotely with students to observe suspected variable stars and to assist in cataloguing them properly. Access to and control of his remote

[1] *Variable stars* are stars that change brightness. The changes in brightness of these stars can range from a thousandth of a magnitude to as much as twenty magnitudes over periods of a fraction of a second to years, depending on the type of variable star.

[2] Red Giants are stars that have completed the consumption of hydrogen in their cores and have left the main sequence.

[3] Magnitude is a logarithmic scale designed to measure the brightness of celestial bodies, commonly stars. The lower the magnitude, the brighter the object; the higher the magnitude, the fainter the object.

Figure 1 — The Bathurst computer-controlled telescope.

telescope is available from any personal computer that has installed *Star MX5* software, which is used to measure the brightness using differential photometry. By creating a remote desktop connection to the telescope, the user can control the telescope using the required software. Two cameras on the telescope provide the user with different views of the same image. One camera looks through the telescope lens, magnifying the image of the desired object(s), while the other camera is placed on top of the telescope to give the user an image through a wide-angle lens pointed at the same area of the sky as the telescope.

Choosing the Suspected Variable Star

When choosing the suspected variable star for the investigation, there were several criteria the star had to meet:

- The star was required to be about 45 degrees above the Bathurst night horizon and able to be photographed for a minimum of 4 weeks
- The star needed to be rising around 5:00 p.m. (in Bathurst) so that it would be high enough by 9:00 p.m. to be accurately photographed
- The magnitude of the suspected variable star needed to be between 9 and 10 in order to be photographed with a relatively short exposure time
- At least one comparison non-variable star with a magnitude between 9 and 10 would be needed to make brightness comparisons (two comparison stars are better than one).

Out of several potential candidates for experimentation, one star was chosen that met the criteria listed above. It was named SAO 154490. It is at a distance of 109.71 light-years away in the constellation Hydra. This suspected variable star had two acceptable comparison stars present in the field of view, GSC 5441:529 and SAO 154486.

Figure 2 — Image of Hydra, the constellation with the position of SAO 154490 indicated.

Figure 3 — Image of Suspected Variable Star (circled in red) and comparison stars (circled in blue).

Measuring Star Magnitude

Dr. McKinnon acquires the digital images of the student's chosen target through his backyard telescope. Four images are taken at each observation and then forwarded to the student responsible for observing the star. These exposures consist of the straight image, the bias image, the dark image, and the flat-field image. The straight image is a straight-forward exposure of the object that contains information about the light coming from the objects in the photograph, plus other components derived from the CCD chip and its electronics that complicate the interpretation of the brightness measurement. The bias exposure characterizes the small voltage applied to the CCD chip, which is measured by a "zero second" (very short) exposure. By subtracting the bias frame from the straight image, the effect of the camera's electronics is removed.

The third image provided is the dark-field image. It has the same exposure as the straight image. This frame is taken because the CCD chip is not at absolute zero. Because of this, "thermal electrons" are created inside the CCD chip and the

glow from these must be removed from the straight image. The flat-field image is an exposure of a uniformly illuminated object such as a twilight sky or a surface evenly illuminated by lights. This frame is designed to correct for the slight unevenness in sensitivity of each pixel across the CCD array. Once this and the other two "calibration" frames have been properly applied to the straight image, the resulting corrected image is ready for differential photometry — the measured difference in brightness between the comparison stars and the suspected variable star. This entire process is done through *Star MX5*. *Star MX5* may also be used to digitally enhance and observe stars and other objects. Through the program, astronomers are not only able to view digital images of objects in space but also to measure features such as brightness or position.

Results

A total of 15 images were taken over a period of 55 days. It was not possible to take images on 40 nights for several reasons, mainly bad weather within that period. Table 1 provides the results for the changes in brightness that were measured compared to the two comparison stars that are non-variable. It also shows records of the date, time, and magnitudes of the two comparison stars. The results are also shown in Graph 1.

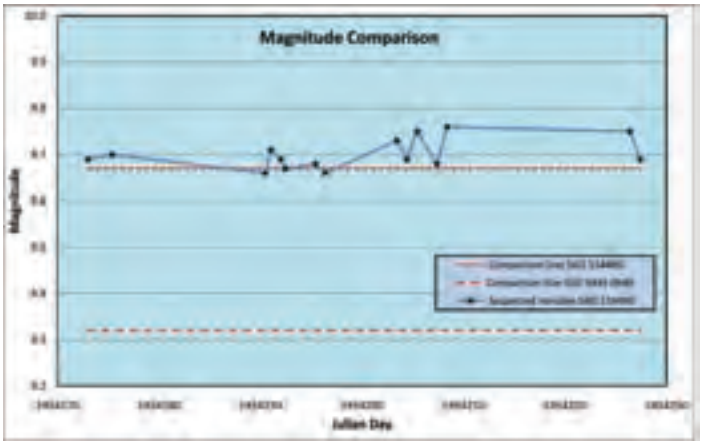

Graph 1 — Light variation of the target star and two comparison stars.

Table 1 — Magnitudes and difference in magnitude of the suspected variable SAO 154490 with the comparison stars SAO 154486 and GSC 5441:529, as measured on 15 occurrences. The derived magnitude of SAO 154490 is the same for either of the comparison stars.

Discussion

The purposes and goals of this analysis were:

1. to observe and record patterns of a suspected variable star using a remotely controlled telescope;
2. to determine whether it is or isn't a true variable star;
3. if it proves to be a true variable star, to determine what type of variable star it is by studying the nature of the brightness variations;
4. to submit collected data and information to the AAVSO International Database.

In accordance with the main hypothesis, if the suspected variable star is observed to undergo a change in the brightness and magnitude it can be concluded to be a true variable star.

When weighted against both of the comparison non-variable stars' brightness over time, it can be seen that there is hardly any variation in the suspected variable star's magnitude. There is a very minor amount of variation in the results (Table 1), but there does not appear to be enough information to conclude that the target, SAO 154490, is a variable, though a significant variability can be ruled out. A final conclusion cannot be reached at this time.

As a result, the target star will be analyzed further following a similar method that uses a different-sized telescope. This second telescope, a 400-mm refractor mounted on the side of the main 12-inch telescope, will give a larger field of view in which to find unsaturated comparison stars of similar magnitude with which to compare the target star's magnitude. This method should improve the measurement statistics, and may give a better idea of the star's variability.

With regard to purpose 3, there cannot be any discussion on the topic as the target was not found to be a variable star within the limits of the error of measurement.

There were several factors that limited the experiment. A small limitation was the inaccuracy when measuring the magnitudes of the stars. It is not likely it has any bearing on the conclusion of this experiment, since it's unlikely the error was that significant according to the stability of the comparison-star magnitudes. Another limitation was that caused by the weather conditions. Since there were days that the star couldn't be photographed, there is an inconsistency in the pattern of observations amounting to large gaps of time between images. Potentially, this could cause the observer to miss days where the star's magnitude had a greater or lesser variation. The amount of time available was a third limitation to the experiment. If there were more months available to observe the star, more data could be gathered that could possibly have an effect on the final result of the experiment.

The information obtained by investigating the suspected variable star, SAO 154490, has been successful in providing important though inconclusive data. The information will now

be forwarded to the AAVSO (American Association of Variable Star Observers) database of variable stars for cataloguing.

Acknowledgements

Special thanks are due to Associate Professor David McKinnon who assisted me in the investigation of the targeted star by emailing me images of the chosen target and providing his time and knowledge throughout the project. Special thanks are also given to Mr. R. Edwards (a science teacher at West Kildonan Collegiate) who worked with me throughout the project and provided many hours of his time and also advice on how to investigate the star and finalize the write-up. Lastly, special thanks are given to Mr. K. Burr (an English teacher at West Kildonan Collegiate) for helping me by peer editing and critiquing the final write-up, and Mr. D. Edwards for helping me with creating the graphs to include in the final version.

References

Books

McKinnon, David 2004, *Practical Astronomy for Years 7, 8, and 9, Using Online Telescopes in Australian Classrooms - Student Workbook,* Charles Sturt University, Bathurst.

Web sites

Variable Stars: `aavso.org/vstar.`

From Hipparchus to *Hipparcos:* `wwwhip.obspm.fr/hipparcos/SandT/hip-SandT.html`

Types of Variable Stars: `www.aavso.org/vstar/types/shtml`

Variable Stars: `en.wikipedia.org/wiki/Variable_star`

Alaina is in her graduating year of high school, looking to pursue an MBA in university in the fall. In her grade-eleven year, she confronted her physics teacher with her interest in astronomy, and has since been looking for new projects to learn more about the stars. She is planning to continue studying astronomy as both a hobby and a university course. This paper won gold in the Senior Physics category and the Winnipeg Centre's Best Astronomy-Related Project award at the Manitoba Schools Science Symposium this year.

ARE YOU MOVING? IS YOUR ADDRESS CORRECT?

If you are planning to move, or your address is incorrect on the label of your *Journal,* please contact the National Office immediately:

(888) 924-7272 (in Canada)
(416) 924-7973 (outside Canada)
email: nationaloffice@rasc.ca

By changing your address in advance, you will continue to receive all issues of *SkyNews* and the *Observer's Handbook.*

Pixellations II: The Telescope-Camera Connection

by Ian Cameron (icamern@cc.umanitoba.ca) and Jennifer West (westjl@cc.umanitoba.ca), Winnipeg Centre

In our first column (*JRASC* February 2008), we discussed some basic adjustments that can be made once the image has been acquired. This time we will take a critical look at imaging using a particular telescope-camera combination so that we can obtain the best possible result. Not only will the images produced look good but they will also be scientifically useful.

When we take astronomical images, our goal is to detect very faint objects with a large amount of detail. Unfortunately these two goals are contradictory. If we try to detect a very faint object, we would have the most success if all the light from that object were concentrated in a single pixel. However, in such a case, we exclude all detail. On the other hand, when we maximize the detail, we spread the light over more and more pixels, thereby decreasing the amount of light per pixel, and making that light much more difficult to detect.

In practice, the amount of detail that we can detect is limited by the turbulence present in the atmosphere and by the optical characteristics of our telescope. The solution is to select a camera with the *fewest* number of pixels required to take advantage of the full amount of detail available to us, given our location and optical instrument; *i.e.* it is not advantageous to have pixels smaller than our conditions dictate.

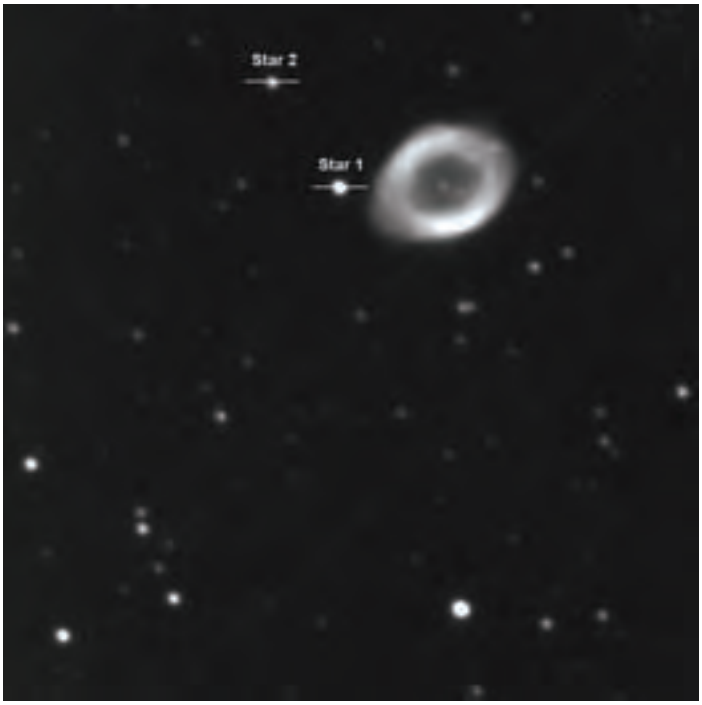

Figure 1 — Three-hundred-second exposure of M57 taken with the University of Manitoba's 16-inch Evans' Telescope and an Apogee AP47 CCD camera. The horizontal lines, which are drawn through the stars labelled Star 1 and Star 2, indicate the position for the plots as shown in Figure 2.

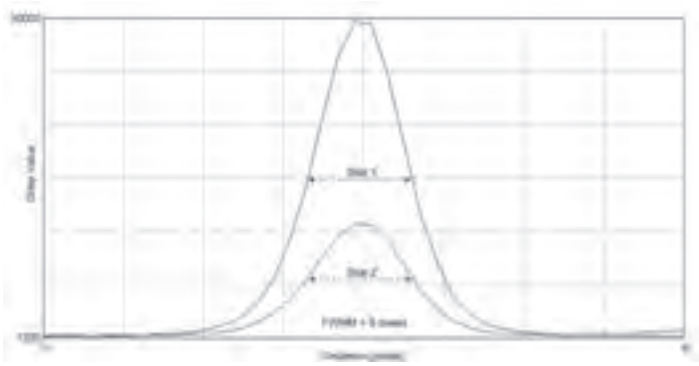

Figure 2 — Profile plots of Star 1 and Star 2 as indicated in Figure 1. Note that the full-width at half-maximum (FWHM) for both profiles is the same. The FWHM is determined by the optical system and the atmospheric conditions, thus it is an invariant quantity across an image.

We will need to make a number of measurements. and the image-analysis package, *ImageJ* (mentioned in the December 2006 *Journal*), allows us to do this easily. Open one of your images in *ImageJ* and have a look at a reasonably bright star near the centre of the field. We are using a monochrome 16-bit image of M57 (Fig. 1). Select the line tool and draw a short line, ensuring that it passes through the centre of the star image (Star 1 in Fig. 1). From the Analyze menu, select Plot Profile. A cross-section of the star image will show in the plot (Fig. 2). Do the same for a somewhat fainter star (Star 2 in Fig. 1 and Fig. 2). You will notice, apart from the scale difference, that the overall shape is the same in both cases. The shape of the profile is a consequence of the optics and the atmospheric seeing. Since a star is essentially a point source, the profile of the star image is referred to as the point spread function (psf). Using our plots, we can easily make some measurements that can give us an indication of the quality of our images. For this application, you should ensure that the pixel values are reasonably below the maximum value possible (a characteristic of your camera). We use the same line length to make visual comparison of our plots easier.

We are going to measure a quantity called the full-width half-maximum (FWHM). If we take the halfway point between the base of the profile and its peak, and measure from one side of the curve to the next, we have a quantity that is *independent* of the brightness of the star we choose (see Fig. 2). If you take the measurements for your two stars, you should find that your two values agree fairly well. The FWHM will give you an indication of the atmospheric seeing. If you happen to be observing during a night when you notice that the seeing improves, you should be able to confirm your suspicion by measuring the FWHM for the earlier and later exposures. The full-width half-maximum can also be used to check on your focus. Though the value of the FWHM will vary over short time scales because of the variation in the atmospheric seeing, you would notice a minimum value for this quantity at best focus. If you are interested in combining images, then knowledge of the FWHM will allow you to decide which images should be used.

If our telescope-camera combination is well "matched," then we have satisfied the condition that we discussed in the previous paragraphs; *i.e.* that we are using the fewest number of pixels required to take advantage of the full amount of detail attainable given the atmospheric seeing at your location. So how do we determine this number? If we have a look at our star profiles (Fig. 2), we see that the FWHM is 6 pixels. This is more than adequate to delineate the profile. Sampling theory indicates that we need a FWHM of *at least* 2 pixels in order to reproduce properly the detail in an image. Since we have a FWHM of 6 pixels, our image is oversampled. Undersampled images will show star images as square blocks, as illustrated in Figure 3. For bright objects such as planets we would deliberately oversample, while for fainter objects the optimal scenario is a matched system with maximum sensitivity. Oversampling ensures that we can do image processing procedures, such as sharpening, with confidence.

Usually the atmospheric seeing is expressed in arcseconds, so we are really interested in how much sky the individual pixels see. You will need to know the actual physical size of the pixels in your camera and also the image scale of your telescope (see Table 1 for typical values). The image scale of your optical system is simply the reciprocal focal length of your telescope (in millimetres) multiplied by 206,265″ (the number of arcseconds in a radian). You could also measure the image scale using *ImageJ* by measuring the distance in pixels between two stars of known separation.

Consider the use of a typical camera, where the pixels are 7.2 microns (0.0072 millimetres) square, and a telescope that has a 4000-mm focal length. The image scale is 206,265″/4000 mm or 51.6″/mm. We can see that what one pixel sees on the sky is 51.6″/mm × 0.0072 mm/pixel = 0.371″/pixel. Our values for the FWHM have so far been expressed in terms of pixels and now we can convert them to arcseconds. Therefore, a FWHM of 10 pixels becomes 3.7 arcseconds, which is an indication of the seeing in an image. At our location here in Winnipeg at the bottom of a river valley, the typical seeing is much worse at ~6 arcseconds.

Figure 3 — Thirty-second exposure taken with a Canon 20Da and a 15-mm fisheye lens at ISO 1600 that shows undersampled star images. The highlighted circular region shows a portion of the image zoomed to show actual pixels. This image shows the Milky Way and the University of Manitoba's Glenlea Astronomical Observatory.

The ideas introduced in this column we will find useful in later discussions. Next time we will discuss the merits of single long-exposure images vs. combining multiple short-exposure images.

Atmospheric Seeing=4 arcseconds								
Telescope Aperture(in)	6	6	8	8	10	10	12	12
Focal Ratio	f/5	f/8	f/6	f/10	f/6	f/10	f/6	f/10
Image Scale (arcsec/mm)	271	169	169	102	135	81	113	68
Matched Pixel Size (microns)	7	12	12	20	15	25	18	30

Table 1 — Typical values for telescope apertures/focal ratios and the corresponding image scales of those systems. Assuming atmospheric seeing of 4″, the optimally matched pixel size for each system is also indicated.

The Chris Graham Robotic Telescope

by Craig Breckenridge, Vancouver Centre (craig.breckenridge@shaw.ca)

Back in early 2005, an individual approached some of the executives of Vancouver Centre to see if there would be any interest in participating in a remote telescope project. Needless to say, Vancouver Council thought this would be an excellent opportunity to bring the latest technologies in remote telescope operation to our membership. The initial planning meetings with Chris Graham, the equipment owner, and some key Vancouver Centre members were held and an agreement in principle was worked out: Chris would provide the equipment and the telescope software and the RASCVC would provide some setup expertise, operational labour, and processing experience. It was a match that would evolve over time, with both sides learning a great deal about remote telescope operation.

The initial setup was located in the New Mexico Skies (NMS) compound on top of Mount Joy, near Cloudcroft, New Mexico. The site is at 7300 feet elevation with latitude of 32°54´ N and longitude of 105°32´ W (Google Earth is quite high resolution in that area so it's easy to pick out the domes). The 20-inch f/8.1 RCOS Ritchey-Chrétien telescope was on a Paramount MME and controlled with *TheSky,* DC3 Dreams' *Astronomer's Control Panel,* and DC3 Dreams' *Scheduler*. We used *Maxim DL* to control the original Apogee Alta U42 back-thinned camera with an 8-position filter wheel. The whole telescope was housed in a 15-foot Technical Innovations Pro Dome that was controlled by *Digital Dome Works.* It wasn't too long before the camera was changed to a SBIG 6303E with the AO7 adaptive-optics package, and control of the dome was turned over to the DC3 Dreams software.

The observatory was set up and the learning curves worked through by a relatively small group that formed the CGRT Operations Committee. The setup was fairly complicated to start with, and we had to overcome a large number of difficulties to understand the route required to make everything function as it should. We did struggle through it all and in the end we were able to script most of the operations so that it became quite simple to organize an observing session, perform the run, and transfer all the data. We had scripted dusk, dome, and dawn flats and were able to take hundreds of gigabytes of data each night. Transfer of the data from the NMS computer to our own FTP server was also scripted to take place during the daytime when bandwidth to operate the scopes was not at a premium. We had even reached the point where DC3 Dreams' *Scheduler* was being utilized for almost completely robotic operation. I say "almost," since we did have some concerns about leaving the scope to run without someone monitoring it across the Internet. And then the bad weather came....

We struggled with bad weather for over a year, only able to operate the scope three or four times in the months from October through December 2007. This was heartbreaking to say the least, and the rent for the compound was very expensive for the small amount of time we could actually use the scope. When New Mexico Skies started up their Pingelly, Western Australia operation in early September, Chris jumped at the opportunity and placed a great telescope in that facility as well. Setup of this new facility consumed the bad-weather months in New Mexico and we were soon treated to southern skies and a wealth of new objects to observe. This led to some hard decisions on the part of equipment owner Chris, as operating

Figure 0 — The Chris Graham Remote Telescope in Pingelly. Photo by Mike Rice.

Figure 1 — eta Carina – One of the brightest nebulae in the sky, but visible only from the southern hemisphere. Taken by the author.

Figure 2 — The familiar shape of the Lagoon Nebula, M8. Image captured by Bob Parry.

two telescopes was a bit more then he could justify spending for what had become an expensive hobby.

The bad weather in New Mexico, combined with the rapid success of the Pingelly operation, brought about a rather substantial change to the CGRT program over the first few months of 2008. In January, I advised the Centre membership that Chris would be winding down the operations in New Mexico by the end of March due in large part to the rather unfavourable weather we had been experiencing over the last year. While this was a bit of a letdown, as we had just managed to learn the operation of *Scheduler,* the CGRT Committee felt that Chris was well justified, as the scope was quite underutilized. We had mastered the issues that arose during normal operation and, if it wasn't for the weather's unpredictability, we could have made the entire operation truly robotic, run only through scripts generated largely by Chris.

In the middle of February, Chris received an offer that he couldn't refuse for the purchase of the entire operation in New Mexico. Since we had been planning to shut the scope down at the end of March, this was only a little earlier than originally planned. The Pingelly operation would be kept running so the RASCVC still has access through the CGRT program to an excellent imaging system (more on this later). The Pingelly site complements Vancouver weather-wise, with their worst observing during the summer when we get our best, and vice versa. There is an added bonus in that we can operate the Pingelly telescope from about 3:00 a.m. to 11:00 a.m., Pacific time. No need to sit up all night to perform an observing run when you can do it over morning coffee! It also makes for very enjoyable Saturday morning get-togethers when a bunch of us can meet at someone's house and have a group imaging session. It's also possible to have operators in multiple locations connected at the same time, provided they run a chat session to coordinate control. This has worked very nicely a couple of times.

Figure 3 — M46 with its elusive planetary nebula companion. Image acquired by the author.

Figure 4 — Exotic NGC 650 acquired by Wayne Lyons.

The Pingelly telescope is an excellent wide-field instrument that has provided us with some great images already — and we are just getting started. Operation of the scope is manual right now as there is a limit to the amount of bandwidth we can use from Western Australia. Pingelly is about 200 km southeast of Perth, and so is a bit of a rural area. The latitude and longitude are 32°31′ S and 117°05′ E. Unfortunately *Google Earth* does not have very high resolution in the area. While we could easily run the scope with the scripts developed for New Mexico, we don't have enough bandwidth to transmit the amount of data that is collected to our FTP servers. Each image is over 12 MB and that doesn't change regardless of exposure time. A single colour image takes a luminance, red, blue, and green exposure. This adds up to over 48 MB and that doesn't count the required darks, biases, and flats!

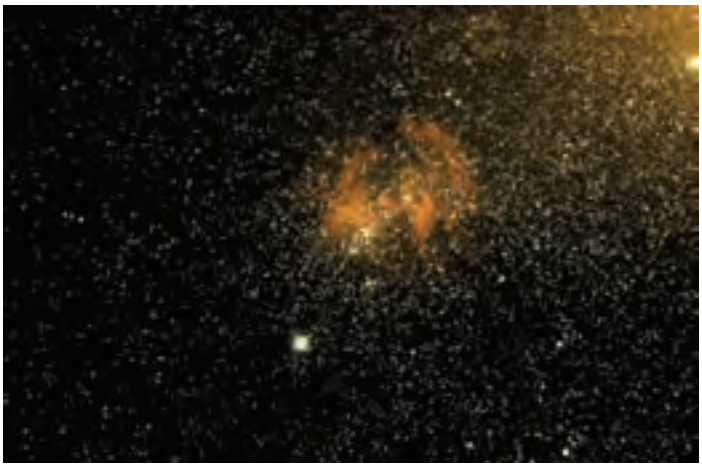

Figure 5 — The Running Chicken nebula acquired by the author.

The Pingelly telescope is housed in a Pod. This is a large roll-off-roof building that houses several remote telescopes. The biggest change for us is not having to worry about controlling a dome and the safety in knowing that the building is manned and not just sitting there waiting for bad weather to roll in. The telescope is a Takahashi Epsilon 210 and is mounted on a Paramount MME German Equatorial Mount. Currently we are using a SBIG STL-6303E Class 1 camera (2k × 3k 9-micron pixels) and a SBIG 5-position filter wheel with R, G, B, L, and Hα filters installed. We also have the AO7 Adaptive Optics package installed. This makes an amazing difference when it's turned on. Chris has been contemplating changing the camera to a SBIG ST-4000XCM (2k × 2k pixels), but hasn't made that decision yet.

We are controlling the scope with *TheSky 6* and the camera with *Maxim DL*. We have DC3 Dreams' *Astronomer's Control Panel* and DC3 Dreams' *Scheduler* installed and will use them once the bandwidth improves. The whole thing runs on a HP XP4300 Dual Core P4 workstation and we use Radmin Remote Desktop to access it. We can fully script everything, but as I said, bandwidth for the transmission of data becomes an issue for the imagery we are capable of collecting in an observing session.

Figure 6 — The Witch-Head Nebula, complete with interloping aircraft – one of the perils of long-exposure photography. Photo by Chris Graham.

Data for images are downloaded from Pingelly to either our PC computer or our Linux FTP server, both of which are located at Simon Fraser University (SFU) in Burnaby. Members can access the data there by requesting access from the CGRT Committee. In the very near future, once we finalize the transfer scripts, we will be transferring data from the SFU computers to the Canadian Astronomical Database Centre at the Hertzberg Institute for Astrophysics (located at the Dominion Astrophysical Observatory on Vancouver Island). The images will then become available to the public and all RASC members. All flats, bias, and dark frames will also be kept current at the CADC so that members and the public can try their hand at processing the images.

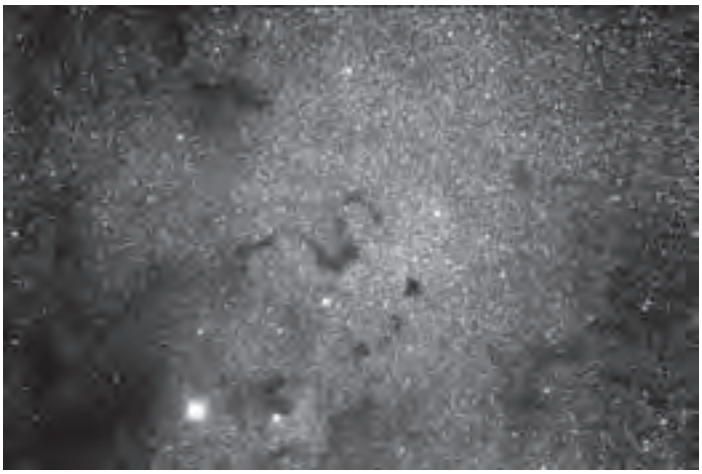

Figure 7 — A monochrome image of the Snake Nebula by Bob Parry and Pomponia Martinez.

The exposures for all the images that accompany this article are 30-seconds or less. Processing was done by Chris Graham, Wayne Lyons, Bob Parry, or Craig Breckenridge. These are just quickly processed images; we have several hundred GB of images available for processing by members if they choose.

All RASC members are invited to participate in the project by joining the CGRT forum at `www.gcrt.ca` where we have a wiki, a forum for discussion, and an event calendar to book time on the scope. Operation of the scope is limited to Vancouver Centre members at the present time but this may be opened up later, once full robotic operation is possible again. A photo gallery is in the works and is partially set up at this time. Any member of the RASC may request that imaging runs be performed on their behalf by contacting the CGRT Committee either through the Web site or via email to Vancouver Centre Council. Members that want to try their hand at processing the data already on

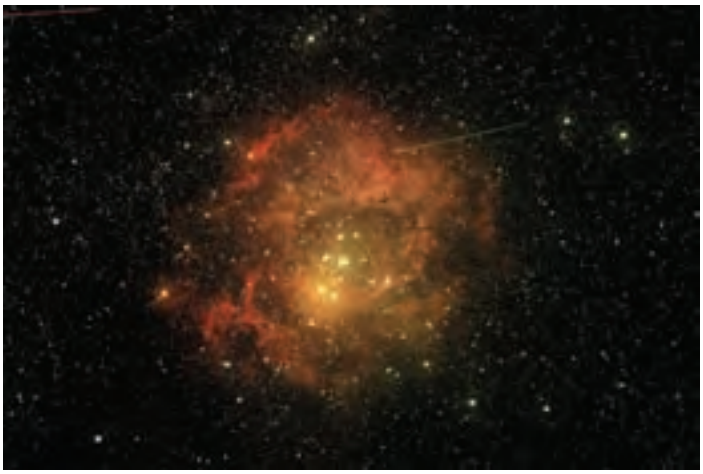

Figure 8 — The Rosette Nebula by Chris Graham (with satellite visitor).

hand can get access to the CGRT FTP server by contacting the CGRT Committee. We have on hand about 300 GB of unprocessed data, including almost all the Messier objects in both colour and black and white.

Craig Breckenridge is the Chairman of the Chris Graham Robotic Telescope project for Vancouver Centre. By day, Craig works at Empire Dynamic Structures and has helped design some of the world's largest telescopes and enclosures. His background is in Mechanical Technology and Structural Design and he has applied his skills to the Keck II enclosure and telescope, the Subaru enclosure, the twin Gemini enclosures, the BLAST telescope, the Atacama Cosmology Telescope, the Gordon McMillan Southam telescope, and currently is working on the Thirty-Metre Telescope and enclosure. His particular interest is in applying his on-site construction experience to achieve a more practical design.

RASC Dark-Sky Program

by Robert Dick, Ottawa Centre (rdick@ccs.carleton.ca)

In the run-up to the International Year of Astronomy in 2009, the RASC has adopted the Dark-Sky Program from the Light-Pollution Abatement Committee (LPAC). This is the Committee's central program to help protect dark sites for amateur astronomy. The defining documents are posted on the RASC-LPA Web site. I would like to introduce these to you so that, with your help, the Program will be in full swing by mid-2009.

The RASC has already recognized six sites as Dark-Sky Preserves. From west to east they are: McDonald Park in B.C., Beaver Hills and Cypress Hills in Alberta and Saskatchewan, Torrance Barrens and Point Pelee in Ontario, and the Mont Mégantic Observatory in Quebec. Several more are on the way.

In the RASC Program, there are two designations. The first is for a great dark site that may be several hours' drive away from an urban centre (such as the six sites above). Visits generally require that you set aside a day or two for serious observing, or you will have a short night and a tired morning.

Figure 1 — Glare versus sky glow – well shielded light fixtures in an urban setting can result in a reasonable sky for stargazing. But even a single unshielded fixture at a good site will ruin the site for astronomy.

These "Dark-Sky Preserves" need preservation. The managers of great astronomy sites are under pressure to cater to the public. In the past, few of them understood the impact of light pollution so they thought more light would help their park. The RASC Dark-Sky Program provides the information they need to make the case for restricted lighting.

But you may think the idea of preserving a dark site is hopeless. Not so! Parks Canada has adopted as "Best Practice" the same lighting protocol that is in the RASC *Guidelines for Outdoor Lighting*, and park managers are now taking a personal interest in protecting their sites from the surge of light pollution. Speak to park managers and you may be surprised by the support and interest you will

Figure 2 — Starfest 2007 – Dark accessible sites are becoming rare and need to be protected.

Figure 3 — Urban Backyard – Neighbour's pesky lights can ruin a good view of an expansive sky.

Figure 4 — LP from a rural hamlet – a few simple shields will reduce the glare and allow the saving of electricity

attract. Federal, provincial, and private parks in your area are prime candidates for Dark-Sky Preserves.

The second type of site is the Urban Star Park. It can be much closer to your city, and may take less than an hour to reach. Or, it may be a municipal park in your neighbourhood. Urban Star Parks are easily accessible for evening observing, public star parties, and getting your evening fix of starlight.

But the closer these sites are to civilization, the greater the chance of unshielded lighting. The glare from a single fixture can wipe out the stars seen under even the darkest sky (see Figure 1). By shielding all lighting visible from within the site, we can turn a park that is abandoned after hours and useless for stargazing into an area fit for celestial solitude.

Admittedly, a site that is close to an urban area will have sky glow, but as long as all the light fixtures visible from the site are well shielded and are set to provide low-level illumination, we will be able to see 4th- to 5th-magnitude stars. This is usually dark enough for people to be guided through the constellations, and its convenience can draw the public in droves to advertised observing sessions.

For the program to protect more sites, we need the help of RASC members. Don't worry — it won't cost any money. In many cases the program will eliminate the apparent need to spend money on lighting or it will reduce the electricity that would otherwise be used.

To help protect these areas from the invasion of artificial lighting requires more than an individual's passionate cry for darkness. It helps if the site is recognized by a national body as a site worth protecting from light trespass and sky glow.

The RASC Dark-Sky Program has been developed to provide this kind of recognition. What we need are sites with good or acceptable astronomical conditions. The best people to identify these sites are you — our members. The information in the program will help you speak to park managers. It is much easier to maintain a good site than it is to correct a bad site. So start now to keep what we have and make other sites better. Recognition by the RASC may tip the scale in the favour of darkness.

Robert Dick has been an advocate against light pollution (LP) for over two decades in the selfish attempt to protect his large observatory in eastern Ontario. He began his formal LP work by creating the Ottawa LP Program that has been adapted for the national RASC Light-Pollution Abatement Program. He teaches astronomy and spacecraft engineering at Carleton University in Ottawa.

The CASTOR "Sputnik 50th Anniversary Satellite-Tracking Bonanza": Project Overview and Preliminary Analysis

by Michael A. Earl, Ottawa Centre (mikeearl@castor2.ca)

Introduction

On 1957 October 4, the Soviet Union launched Sputnik 1, the Earth's first artificial satellite. Today, 50 years later, nearly 13,000 individual man-made objects orbit the Earth in the form of payloads, spent rockets, and an abundance of debris.

Last year, the Canadian Satellite Tracking and Orbit Research (CASTOR) project celebrated this monumental anniversary by optically detecting and tracking over 2000 artificial satellites. This is the first time anyone independent of government or military has completed an ambitious project of this nature. The project began on 2007 January 1 and concluded on December 31. During the year, 50,000 images containing 2050 satellites were obtained with a single SBIG ST-9XE CCD camera.

This project was also designed to be a preliminary survey of satellites that could be detected with standard astronomical equipment: GOTO telescopes with apertures of 20 and 28 cm (8 and 11 inches) and a CCD camera with a minimum quantum efficiency of 50 percent. Currently, all of the images collected during 2007 are being analyzed for every possible piece of data that can be extracted.

This paper gives an overview of the project and presents the results of the preliminary analyses carried out during the first quarter of 2008.

Project Overview

Target Satellites

CASTOR detected and tracked satellites in four critical orbit types:

Low Earth Orbit (LEO) satellites were tracked from 2007 January 1 to March 31. For this project, LEO satellites were defined to have a maximum average orbit altitude of 1700 kilometres (a maximum orbital period of 2 hours). This orbit type includes all Sun-synchronous (polar-orbiting) satellites.

Mid Earth Orbit (MEO) satellites were tracked from 2007 April 1 to June 30. For this project, MEO satellites were defined to have an average orbit altitude between 1700 and 35,500 kilometres (orbital periods between 2 hours and 24 hours). This orbit type includes all the semi-synchronous GPS and Russian Molniya-type satellites.

Geosynchronous satellites (GEO) were tracked from 2007 July 1 to August 31. For this project, GEO satellites were defined to have an average altitude of between 35,500 and 36,500 kilometres (orbit period of nearly one sidereal day). This orbit type includes the satellite-radio and satellite-television satellites currently servicing North, Central, and South America.

High Earth Orbit (HEO) and new satellites of the types defined above were tracked from 2007 September 1 to December 31. For this project, HEO satellites were defined to have a minimum average orbit altitude of 36,500 kilometres (an orbit period greater than one sidereal day). This orbit type includes all of the super-synchronous satellites.

Equipment Used

Hardware

- A NexStar 11 GPS 26-cm (11-inch) GOTO telescope (2800-mm focal length) was used as the main telescope in the project.
- A NexStar 8i SE 20-cm (8-inch) GOTO telescope (2100-mm focal length) operated as a portable and as a backup telescope
- A Rikenon 50-mm camera lens for wide-field imaging.
- A SBIG ST-9XE CCD camera (512×512 pixels, 20 microns each) was used for all imaging during the project.
- An Astro Power Cube (built by CASTOR) that housed all of the power supplies for the hardware.
- One Compaq Presario 2199CA notebook computer controlled all telescopes and the CCD camera.

Software

TLESort (created by CASTOR) organized all orbit elements of the candidate satellites into their corresponding orbit types (LEO, MEO, GEO, and HEO). Software Bisque's *TheSky Version 5* was used to predict satellite locations and control both telescopes, and Software Bisque's *CCDSoft Version 5* software was used to control the CCD camera and will be the main tool for astrometric and photometric analyses of all 50,000 images in 2008.

Satellite-Tracking Logistics

All LEO satellites were tracked using an SBIG ST-9XE CCD fitted with a Rikenon 50-mm lens, piggybacked on the NexStar 11 telescope. The camera had a field of view (FOV) of 11.26

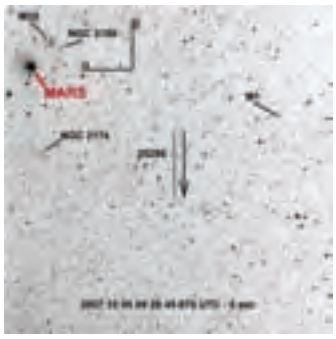

Figure 1 — A CASTOR image of the *Iridium* 62 (LEO) satellite (CASTOR #1734; NORAD #25285). This image includes the planet Mars, clusters M35 and NGC 2158, nebula NGC 2174 and the Crab Nebula (M1). The compass directions indicate increasing Right Ascension and increasing Declination. The arrow indicates the satellite's apparent direction of travel. This is a negative of the original 5-second CASTOR image obtained at 09:28:45.670 UTC 2007 October 5. The limiting stellar magnitude is 10.

Figure 2 — A CASTOR image of two Russian "*Glonass*" GPS (MEO) satellites (CASTOR #s 0558 and 0559; NORAD #s 23735 and 23620 respectively) obtained with the NexStar 8i telescope and SBIG ST-9XE CCD. The compass directions indicate increasing Right Ascension and increasing Declination. The arrow indicates the direction of travel of both satellites.

Figure 3 — A CASTOR image of the Japanese *Superbird* B1 (GEO) satellite (CASTOR #1229; NORAD #21893) obtained with the NexStar 11 telescope and SBIG ST-9XE CCD. This satellite was undergoing a brilliant sunlight reflection during the exposure. The compass directions indicate increasing Right Ascension and increasing Declination. The arrow indicates the satellite's apparent direction of travel. This is a negative of the original 10-second CASTOR image obtained at 05:10:25.670 UTC 2007 July 23. The limiting stellar magnitude is 18.

degrees and angular resolution of 1.32 arcminutes per pixel. A typical CASTOR LEO image is illustrated in Figure 1.

All MEO and GEO satellites were tracked using either the NexStar 8i or the NexStar 11 telescopes with the ST-9XE CCD at prime focus. The FOV and angular resolution for the NexStar 8i were 18.73 arcminutes and 2.195 arcseconds per pixel, respectively. The FOV and angular resolution for the NexStar 11 were 13.33 arcminutes and 1.56 arcseconds per pixel, respectively. A CASTOR MEO image is illustrated in Figure 2 and a CASTOR GEO image is illustrated in Figure 3.

All HEO satellites were tracked using the NexStar 11 GPS telescope with the ST-9XE CCD at prime focus. A CASTOR HEO image is illustrated in Figure 4.

Figure 4 — A CASTOR image of the Russian X-Ray Observatory *Astron* (HEO) satellite (CASTOR #0978; NORAD #13901) (circled) obtained with the NexStar 11 telescope and SBIG ST-9XE CCD. This satellite was the furthest that CASTOR detected in 2007, with a range (distance) of nearly 196,000 kilometres. Galaxy NGC 5387 and a 2MASX survey galaxy also appear. The compass directions indicate increasing Right Ascension and increasing Declination. The arrow indicates the satellite's apparent direction of travel. This is a negative of the original 30-second CASTOR image obtained at 04:37:25.670 UTC 2007 June 13. The limiting stellar magnitude is 18.

Preliminary Analysis

Unique Satellites Tracked per Month

Figure 5 illustrates the number of unique satellites that CASTOR detected each month of 2007. "Unique" refers to satellites not already detected in any of the preceding months.

Total and Detected Satellites by Orbit Type

Figure 6 (left) illustrates the percentage of total satellites in each orbit type with respect to the estimated total number of satellites currently in orbit (12,800) while Figure 6 (right) shows the percent of detected satellites of each orbit type with respect to the total number of detected satellites (2050). Figure 7 illustrates the percentage of detected satellite types in each orbit with respect to the total number of satellites in each kind of orbit (LEO, MEO, GEO, and HEO respectively).

Continued on page 156…

Pen & Pixel

M13 by Stef Cancelli. This gorgeous photo of our brightest northern hemisphere globular was taken from Toronto on May 17 and 25. Stef used a VC200L at f/9 giving a focal length of 1800 mm. Exposures were 55:60:60:60 minutes for an unbinned luminance and binned R:G:B images. With its older red stars spread on a background of blue, the cluster almost seems alive.

Ottawa's Rolf Meier captured his first Saturn image of the year and his first proper RGB image of the planet on 2008 April 23 at 01:56 UT using a C14 telescope at f/47 and a Lumenera SKYnyx 2-0 camera. He notes that seeing was unusually poor. The recent white spot on the planet can be seen in the upper left of the disc. Saturn's rings are now flattening rapidly as the planet approaches the date at which the Earth crosses the ring plane and the rings "disappear" for a short time.

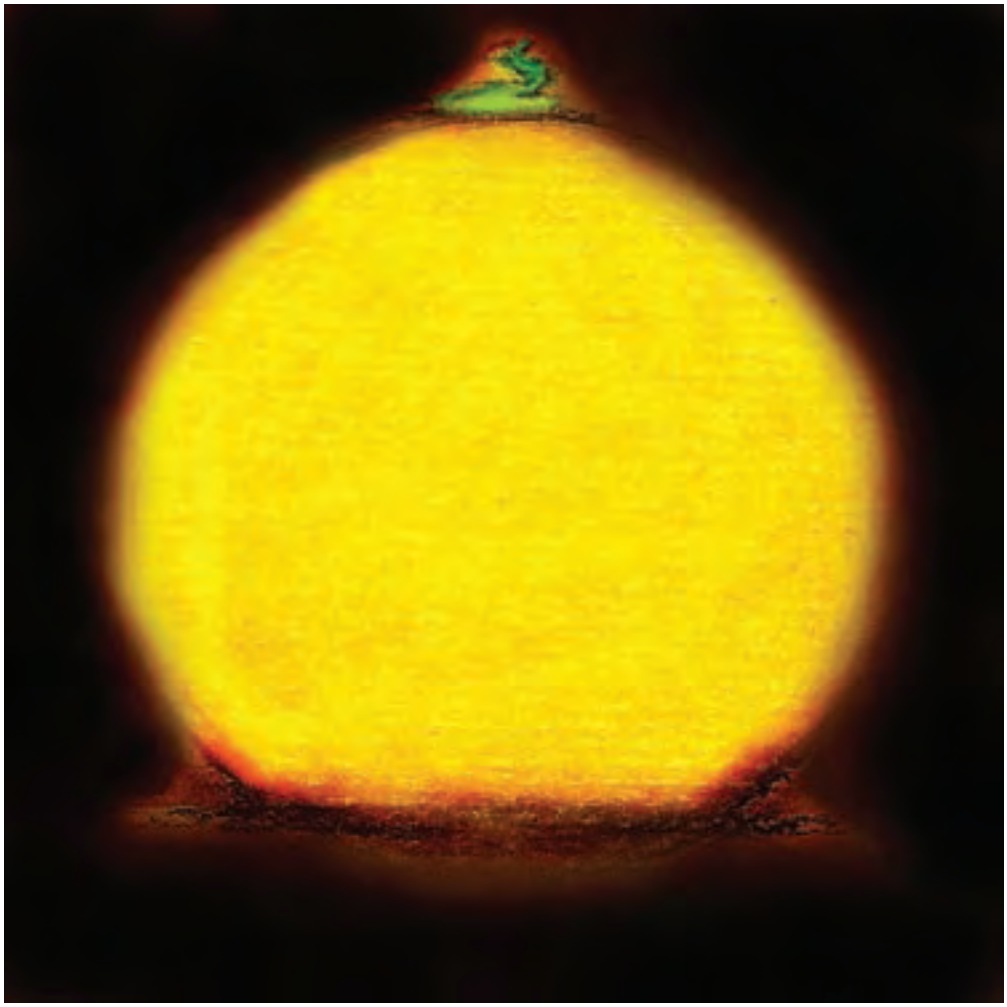

This drawing by Toronto's Randall Rosenfeld records one of the more common varieties of the green flash, the mock mirage. Green flash phenomena are effects of atmospheric refraction, which may be seen fleetingly at sunrise and sunset, if conditions are favourable. Randall reports that the flash was observed at sunset on March 16 from an elevated position in Toronto with a clear view to the western horizon (a rare circumstance!). Equipment: 8-cm f/6 semi-apo refractor, an objective filter of Baader Astro-Solar Safety film, a 25-mm Plössl eyepiece, and a No. 12 Wratten filter.

Steve Irvine took both of these photos with exactly the same photographic equipment – the difference in size is because the October Moon was 53,000 km closer at perigee than the May Moon was at apogee. The Moon also wobbles slightly in its orbit, an effect called libration. The May Moon shows some craters in the north that can't be seen in the October Moon, showing that the May Moon was tilted slightly forward in the north. Steve does most of his photography from his home on the Bruce Peninsula in southern Ontario.

…Continued from page 153

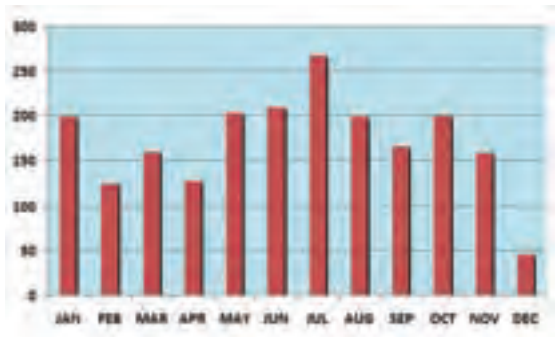

Figure 5 — The number of unique satellites CASTOR detected per month in 2007. The low number in December was caused by inclement weather.

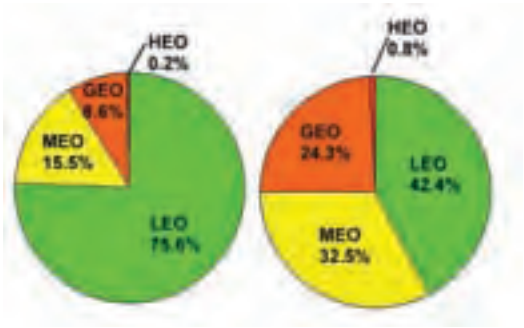

Figure 6 — Left: The percentage of total satellites in each orbit type with respect to the estimated total number of satellites currently in orbit (12,800). Note the dominant LEO percentage. Right: The percentage of the number of detected satellites in each orbit type with respect to the total number of detected satellites (2050).

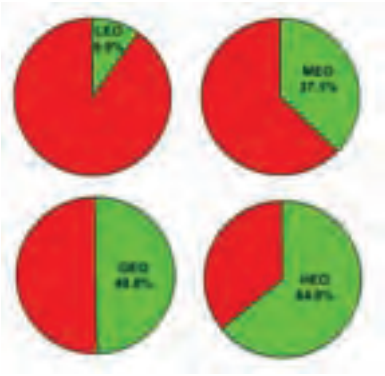

Figure 7 — The percentage of the total number of LEO, MEO, GEO, and HEO satellites detected.

Detected Satellites by Country

Figure 8 illustrates the percentage of detected satellites from each country with respect to the total number of satellites detected (2050).

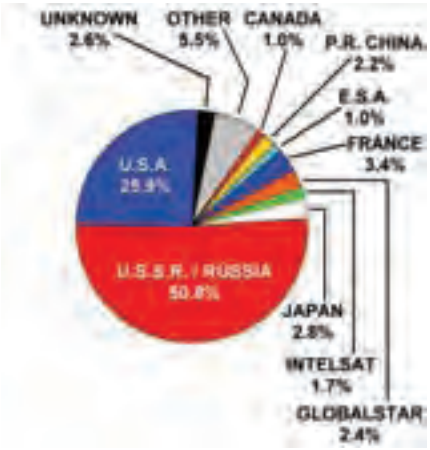

Figure 8 — Percentages of the satellites detected by country of origin with respect to the total number of satellites detected (2050). In several instances, private companies (*Globalstar* and *Intelsat*) are indicated. "Other" refers to the remaining countries that represented less than one percent of the overall number detected. "Unknown" refers to those detected satellites that could not be positively identified.

Detected Satellite by Category

Detected satellites were binned into three categories: "payloads," "rocket bodies," and "debris." "Rocket bodies" mainly refers to spent rockets in orbit. "Debris" refers to small fragments of payloads or rocket bodies. "Payloads" refers to those satellites not considered rocket bodies or debris.

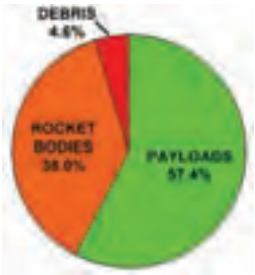

Figure 9 — Percentages of the detected payloads, rocket bodies, and debris with respect to the total number of detected satellites (2050). Note the small percentage of debris that was detected.

Notable Satellites Detected

Of the 2050 unique satellites that were tracked by CASTOR in 2007, there were some that were of special interest:

***The International Space Station* (ISS; Alpha; CASTOR #0026; NORAD #25544):** The first internationally constructed space station of the Earth;

***Fengyun 1C* Debris (CASTOR #0141; NORAD #29933):** One single piece of the more than 2000 pieces of debris left over from the intentional destruction of a Chinese

weather satellite by a Chinese anti-satellite missile;

Telstar 1 **(CASTOR #0466; NORAD #00340):** The first satellite to transmit live transatlantic television broadcasts from North America to Europe and vice-versa;

Giove-A **(Jupiter-A; CASTOR #0467; NORAD #28922):** The first GPS satellite by the European Space Agency (ESA);

Westford Needles **(CASTOR #0575; NORAD #02364):** One of the many pieces of debris left over from the Westford Needles project. This 1960s project involved placing millions of tiny copper needles into space to serve as an artificial ionosphere;

CXO **(Chandra X-Ray Observatory; CASTOR #0976; NORAD #25867):** One of the "Big Four" space observatories launched by NASA, including Hubble, Compton, and Spitzer;

Anik A1 **(Telesat 1; CASTOR #1170; NORAD #06278):** The first GEO satellite for domestic (non-military) use. Built by Telesat Canada;

Celestis 2 **(Ad-Astra; Taurus Rocket; CASTOR #1454; NORAD #25160):** The second memorial spaceflight satellite that contained the cremated remains of loved ones; and

RADARSAT 1 **(CASTOR #1982; NORAD #23710):** Canada's first Earth-observation satellite. This satellite was built by MacDonald, Dettwiler and Associates, Canada.

Conclusions

The 2050 satellites detected by CASTOR constitute 16% (nearly 1/6th) of the estimated 12,800 satellites currently in Earth orbit. This project shows that commercial off-the-shelf small-aperture telescopes and CCD cameras can be utilized to detect and track a significant portion of our current satellite population. Nearly one-tenth of the total number of LEO satellites were detected (Figure 7), though there were several factors that prevented the detection of many of the satellites in this type of orbit:

- LEO satellites orbit very quickly over the Earth's surface. Most of these satellites can cross the observer's sky in 20 minutes or less. In many cases, as one LEO satellite is being tracked, many others are also accessible at the same time but can become inaccessible quickly, before they can be imaged. Additional CCD cameras and larger fields of view would be two solutions to this particular problem. A second survey planned for 2009 will attempt to detect more unique LEO satellites.
- Many LEO satellites are in fact very small debris particles only a few centimetres in size. The apparent angular velocity of a LEO satellite is very fast and travels across the CCD chip very quickly, allowing very little integration time per pixel. Because of this, many LEO satellites invariably have brightness (signal) below the CCD detector's background noise.
- Many LEO satellites are Sun-synchronous, meaning they orbit nearly along the Earth's terminator (night-day divide). Most of these satellites can only be detected optically within the first two hours after sunset or the first two hours before dawn. Some LEO satellites will be within, or in close proximity to, the twilight (or dawn) glow, thereby rendering them nearly invisible to optical equipment.
- Many LEO satellites are simply eclipsed by the Earth. Once the Earth blocks the sunlight to a satellite, it is undetectable by optical means. This reduces the amount of available time that the satellites are accessible by CASTOR.

Over one-third of the total MEO satellites were detected (Figure 7). In most cases, the undetected satellites were either too small or too dim to be detected by CASTOR's optical equipment. Nearly one-half of the total GEO satellites were detected (Figure 7). Although many GEO satellites are very large and bright, there are several factors that can still render them optically undetectable:

- Many GEO satellites reside on the opposite side of the Earth from the CASTOR observing site in Brockville, Ontario, Canada. One solution to this problem is to employ a second CASTOR facility on or near the opposite side of the Earth from Canada to access the remaining detectable GEOs.
- Some GEO satellites are either too small or simply too dim to be optically detected by CASTOR. These mainly come in the form of very small debris particles from old payloads or rocket bodies. This debris would be about 36,000 kilometres in altitude and approximately 500 times (6.8 magnitudes) dimmer than a satellite of the same size at the outer edge of a LEO orbit (1700 km).

Nearly two-thirds of the HEO satellites were detected (Figure 7). This result is not surprising as most of these satellites are very slow moving and large in size. The main reason why *Astron* (Figure 4) was detected at a range of 196,000 km was mainly due to its large size and slow apparent angular velocity that translated into a large pixel integration time on the CCD chip.

The large proportion of Russian and American satellites detected was not surprising as these two nations were the most prolific in satellite launches in the past 50 years. What is surprising is the difference in the percentages of the two countries, despite the fact that at present both countries have nearly the same number of orbiting satellites (approximately 4400 each). This discrepancy might be explained by the fact that the Soviet Union launched extremely massive payloads and

rockets, while the Americans launched much more compact (and less reflective?) payloads and rockets during the Space Race of the latter 20th century. A good example of this is the difference in size between *Sputnik 1* (58 cm) and *Vanguard 1* (16 cm). CASTOR tried but failed to detect *Vanguard 1*.

The third largest number of satellites binned by country (not including "Other") originated in France (Figure 8), due mainly to the very successful Ariane rockets. No doubt, the Chinese percentage would have been much greater had CASTOR been able to detect a greater amount of the debris from the *Fengyun 1C* weather satellite.

The small amount of debris that was detected by CASTOR (Figure 9) is not surprising. CASTOR utilizes small-aperture telescopes and, as a result, most debris will certainly be missed. It is possible that a future analysis will determine possible cross-section (size) limits based on the faintest satellites detected. This data could possibly be used to establish a correlation between the satellites' detected brightness and their radar cross-sections, although there will be numerous factors and variables involved.

The next CASTOR publication will feature the final results of the photometric and astrometric analyses of all 2050 satellites CASTOR detected in 2007.

Plans are underway for a second yearlong CASTOR survey of our Earth-orbiting satellites to begin on the evening of 2009 January 1. This second survey is expected to provide a supplementary CASTOR satellite catalogue in addition to the preliminary 2050 satellites already detected.

Web Resources

Space Track — The Source for Space Surveillance Data — `www.space-track.org`: All up-to-date orbit elements for all 2050 satellites CASTOR detected and tracked in 2007;

Chris Peat's Heavens Above — `www.heavens-above.com` — Preliminary predictions for the naked-eye LEO satellites; and

Mike McCants' Satellite Tracking Web Pages — `www.io.com/~mmccants` — Orbit elements for the notable satellites CASTOR detected and tracked in 2007.

Acknowledgements

A special thanks to the 1st Space Control Squadron (1SPCS) at Cheyenne Mountain (Colorado) for their words of encouragement and their expertise in 2007.

Castor Web Site

To learn more about the CASTOR project and its goals, please visit the CASTOR Web site at `www.castor2.ca`.

Astrocryptic

The solution to last issue's puzzle:

Spin Me Up

by Leslie J. Sage (l.sage@naturedc.com)

Binary asteroids and minor bodies (such as the Pluto-Charon pair) are seen throughout the Solar System. About 15 percent of the main belt and near-Earth asteroids whose diameters are less than 10 km have smaller companions on close circular orbits. The primaries tend to be spinning quite rapidly, and one has been found to have a pronounced equatorial bulge. While tidal encounters with a planet could in principle lead to the formation of a binary from a "rubble pile" asteroid, it turns out that these encounters are even more effective in disrupting them. Collisions in the main belt that lead to catastrophic disruption could produce binaries, but the properties of such binaries would be quite different than what are seen. The trick is to get a mechanism that works both in the main belt and in the near-Earth region. Kevin Walsh and Patrick Michel of the Observatoire de la Côte D'Azur in France, and Derek Richardson of the University of Maryland have now figured out how these binaries are made (see the July 10 issue of *Nature*). A single rubble-pile asteroid is spun up by what is called the "thermal YORP effect" to the break-up speed. Material is ejected from the equatorial region of the asteroid, where it collects in a close, low-eccentricity orbit and subsequently coalesces into a small secondary.

The thermal YORP effect arises from sunlight. The Sun warms the asteroid throughout the "day." The warmer rock on the "sunset" side will radiate more infrared photons than the rock on the "dawn" side. This difference means that there is a net force acting on the asteroid, which over time pumps up the rotation speed. The spin-up time varies with, for example, distance from the Sun, and the size of the body; for kilometre-sized bodies, it is roughly a million years. (The effect also can spin down asteroids and reverse their direction of rotation.) While it was already known that the YORP effect could spin

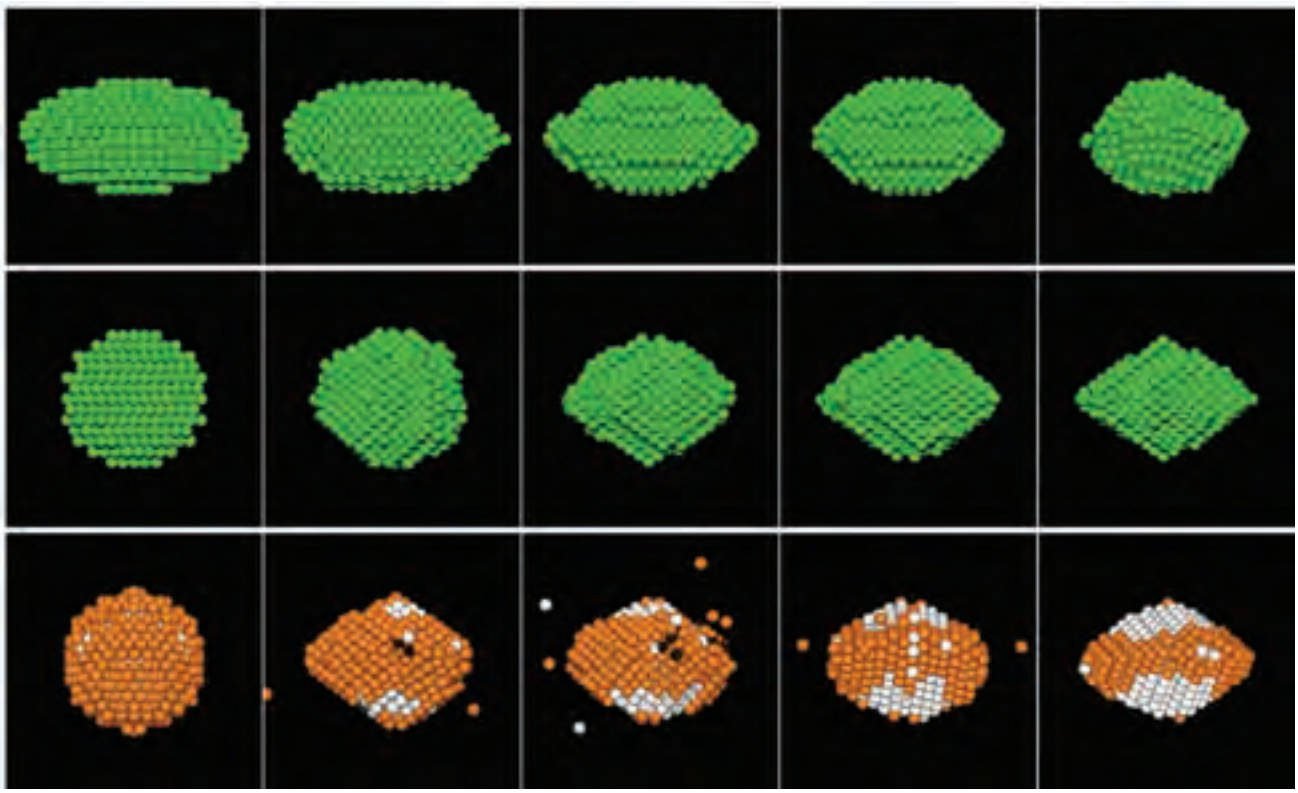

Figure 1 — Evolution of asteroid shapes during spin up. The top row shows the evolution of a prolate body as it is spun up and loses mass. The mass is rapidly re-accreted. The middle and bottom rows show the evolution of an initially spherical body. The orange surface material in the bottom row is gradually replaced near the poles by the white interior material. Figure courtesy of Kevin Walsh and *Nature*.

up asteroids, no one had checked whether the asteroids would lose mass or whether the lost mass could form a companion with the observed properties.

Walsh and his colleagues simulated the spin-up of a rubble-pile asteroid. Such a body is held together only by its own gravity, with no structural strength, and it appears that most kilometre-sized asteroids are rubble piles. One critical parameter in the simulation is the "angle of friction" of the material — this parameter is a measure of how the rubble "flows" under stress. The simulation varied the value of this parameter between one appropriate for a fluid, and one appropriate for terrestrial rocks, and included an intermediate case. They ran the simulations for bodies that were initially spherical and prolate (what you get by spinning up a fluid held together by gravity), and they varied the "bounciness" of the rocks.

They found that as an initially prolate body was spun up, the mass that was ejected went into very low orbits, from which it was easily disturbed by the asymmetrical primary and re-accumulated onto the surface. On the other hand, an initially spherical primary became oblate as rocks migrated from the poles to the equator, and the ejected material rapidly accumulated into a satellite. If the primary's shape was not initially spherical or oblate, satellite formation was delayed until it became oblate. As you might expect, the efficiency of satellite formation dropped rapidly as the stickiness was decreased. A solid core surrounded by loose material forms satellites about as well as a rubble pile, provided that the primary becomes oblate in shape.

The binaries form easily under the right conditions, and can grow (in the simulation) quite large. As no close, large binaries are known, some process must stop the growth of the secondary at some point. Walsh speculates that a YORP effect on the binary as a system (the "binary YORP effect") could be the reason.

Curiously, after the secondary has formed, a good chunk of the surface of the primary asteroid, especially near the poles, turns out to be rock from below the surface. The equatorial region is still mainly original surface material, and of course the secondary is mostly made of surface material. So one way in the future to get a glimpse of the interior of an asteroid will be to look at the poles of the primary in a binary system!

Leslie J. Sage is Senior Editor, Physical Sciences, for Nature Magazine *and a Research Associate in the Astronomy Department at the University of Maryland. He grew up in Burlington, Ontario, where even the bright lights of Toronto did not dim his enthusiasm for astronomy. Currently he studies molecular gas and star formation in galaxies, particularly interacting ones, but is not above looking at a humble planetary object.*

Deep Sky Contemplations

Hunting in the Virgo Cluster

by Doug Hube (jdhube@telus.net) and Warren Finlay (warren.finlay@interbaun.com), Edmonton Centre

Within an area roughly 12½ degrees east-west by 7 degrees north-south centred near RA = 12½^h, DEC = +12°, there are sixteen Messier objects identified as galaxies (Figure 1). Such a concentration cannot be due to chance and, of course, experienced observers will recognize those objects as members of one of the largest clusters of galaxies known: the Virgo Cluster. At a distance of 17 megaparsecs it is the nearest of the large clusters and contains some of the most massive galaxies known, in particular the giant elliptical M87.

The Virgo Cluster has played a pivotal role in many research projects in extragalactic astronomy. In 1926, Shapley and Ames were the first to recognize this concentration of galaxies as a *cluster* of galaxies. Several decades later, de Vaucouleurs identified a population of galaxies that extends from the Virgo Cluster to our Local Group, and proposed the existence of a Local *Super*cluster.

With so many bright galaxies, the Virgo Cluster was one of the first to have its radial velocity determined and relative internal motions investigated. With the cluster at a distance of 17 Mpc, we expect a cosmic recessional velocity

Figure 1 — Position of the Virgo Cluster in the night sky.

Figure 2 — Image of the M84/M86/Markarian Chain region of the Virgo Cluster obtained (and kindly provided) by John Mirtle of the Calgary Centre, using SBIG ST-8XE, SBIG RGB filter set, Takahashi FSQ-106N, 3x20 min L, 2x20 min R, 2x20 min G, 2x20 min B; Wilson Coulee Observatory, Alberta, 2006 April 23.

of approximately 1200 km s^{-1}, close to the midpoint of the measured radial velocities of the individual member galaxies; those velocities range from approximately 40 to 2940 km s^{-1}. That range means that internal velocities of the member galaxies relative to the cluster as a whole, the so-called peculiar velocities, must extend up to at least 1450 km s^{-1}. If the mass of the cluster were no more than the mass of the luminous matter that is observed directly, a galaxy with such a large velocity would escape. Other evidence implies, however, that the cluster is gravitationally bound.

If you had X-ray vision you would observe a bright, diffuse glow throughout the cluster, especially intense in extended regions around the most massive member galaxies. That glow is direct evidence for the presence of a substantial amount of hot, intergalactic gas in the cluster.

If one takes the mass of the luminous material detectable at optical and radio wavelengths and adds to that the mass of the X-ray-luminous intergalactic material, there is still not enough mass to prevent the escape of the most rapidly moving galaxies within the cluster. The conclusion is unavoidable: the cluster contains substantial amounts of dark matter. Once again, our eyes deceive us.

It is well known that our Local Group of galaxies has two centres of sub-clustering: one centred on the Milky Way, the other centred on M31, the Andromeda Galaxy. Not surprisingly given its much larger population, the Virgo Cluster has more: there are at least three well-defined sub-clusters centred on its most massive galaxies, namely M87, M86, and M49.

From our home in the Milky Way, we can observe easily with the unaided eye two neighbouring galaxies: the Large and Small Magellanic Clouds. On a clear, dark night, our giant neighbour M31 is an easy target for those who know where to look. Under exceptional circumstances and with exceptionally good eyesight, the third-largest galaxy within the Local Group, M33, has been detected with the naked eye by a few observers. Can you imagine how marvellous the sky must look for observers — and there *must* be some observers there, must there not — living within galaxies in the Virgo Cluster?

Doug Hube is a professional astronomer actively retired from the University of Alberta, and Associate Editor of this Journal. *Warren Finlay is the author of* Concise Catalog of Deep-Sky Objects: Astrophysical Information for 500 Galaxies, Clusters and Nebulae *(Springer, 2003), and is a professor of mechanical engineering at the University of Alberta.*

Sing we and Chant it!

By Geoff Gaherty, Toronto Centre (geoff@foxmead.ca)

Sing we and chant it
while love doth grant it,
fa la la, etc.

Not long youth lasteth,
and old age hasteth;
now is best leisure
to take our pleasure,
fa la la, etc.

All things invite us
now to delight us,
fa la la, etc.

Hence, care, be packing!
no mirth be lacking!
Let spare no treasure
to live in pleasure,
fa la la, etc.

— Thomas Morley

One of my major non-astronomical interests is early music, and this famous madrigal by Thomas Morley has long been a favourite of mine. I thought I would use it as a jumping off point to talk a bit about the Chant Medal, which I was awarded at this year's General Assembly in Toronto.

My first reaction, when I received notification of my award from Peter Jedicke in an email on April 1, was that it had to be an April Fool's joke. I have known a number of Chant Medallists over the years, and I did not feel I belonged in that league.

The Chant Medal was named in honour of Clarence Augustus Chant, who guided the RASC and the University of Toronto's astronomy department through most of the first half of the 20th century. According to our Web site, "This medal is awarded...to an amateur astronomer resident in Canada on the basis of the value of the work carried out in astronomy and closely allied fields of the original investigation...." To me, this description has always implied some sort of major research project, which was why I was puzzled to receive it. In truth, I am something of an astronomical dilettante, dabbling in many different aspects of astronomy. Later Peter J. explained to me that in his view, the Chant is thought of nowadays as a lifetime achievement award.

Receiving the Chant Medal has caused me to reflect on the Chant Medallists I have known during my life, and how strongly they have influenced me. The first recipient in 1940, a year before my birth, was Bertram J. Topham (1893–1962) of the Toronto Centre.

Figure 1 — Bertram J. Topham at the eyepiece of his refractor.

He was a variable star observer (like me) and used a magnificent 165-mm refractor from his observatory in northwest Toronto. Although I never met him, I spent many evenings observing through his wonderful telescope, which had been purchased by the Montréal Centre a few months before I joined the RASC in 1957. To a teenager with a 4.25-in Newtonian, this was my first close encounter with a *real* telescope! Here is the note in my log of my first visit to the Montréal Centre's observatory on 1957 October 5:

"Tonight I joined the Royal Astronomical Society of Canada for $2.50 (half year). Very impressed with their 6.5″ refractor with drive clock etc...Looked at the Moon through 6.5″ and, although the sky was very hazy, image was very good. I will get my *Observer's Handbook* when I go next time as librarian was not there and Mr. DeKinder could

not find a copy. Borrowed copies of July *Sky & Telescope* and January-June *Strolling Astronomer*. Also got a copy of *Skywards* [sic]."

The Mr. DeKinder mentioned was Frank DeKinder (1892–1970), who received the Chant Medal in 1955 for his decades of regular solar observations for the AAVSO. Frank used to live near his work, and would go home for lunch every day to record sunspots. He later went on to become president of the AAVSO.

At the meeting the following Saturday, I met two important members of the Centre who had been down in Cambridge for the AAVSO annual meeting the previous week: Charles M. Good (the missing librarian) and Isabel K. Williamson (1907–2000), the Montréal Centre's other Chant Medallist and driving force. She had received the Chant Medal in 1948 for her work in organizing and analyzing meteor observations.

Isabel (though none of us ever dared call her anything but "Miss Williamson" to her face) was a "computer" by profession: she was employed in the actuarial department of the Sun Life Assurance Company and spent her working life performing calculations and working with the earliest electronic computers. In astronomy, she was a true "Renaissance woman," who was an expert in all forms of astronomical observation, and a genius at designing training programs and encouraging beginners. Her most famous contribution to astronomy was her creation of the world's first Messier Club in the early 1940s.

Here is a photograph taken at a Centre meeting a few weeks before I joined, which brings back warm memories to me of my earliest days at the Montréal Centre:

Frank DeKinder is standing to the left of the blackboard, and George Wedge and Isabel Williamson are standing to the right. Seated around the table are many "regulars" at the Centre's Saturday night meetings, who would, only a short time later, become some of my closest friends for many years. Frank and Isabel in particular both became mentors to my burgeoning interest in astronomy.

I will return to the subject of later Chanters in my astronomical life in a future column! For the present, I will just add what an incredible honour it is for me to join the "order of the Chant."

Geoff Gaherty is currently celebrating his 50th anniversary as an amateur astronomer and as the 2008 recipient of the Society's Chant Medal. Despite cold in the winter and mosquitoes in the summer, he still manages to pursue a variety of observations, particularly of Jupiter and variable stars. Though technically retired as a computer consultant, he is now getting paid to do astronomy, providing content and technical support for Starry Night Software.

Dial F

by Don Van Akker, Victoria Centre (don@knappett.com)

To be an astroimager you need to be a bit of a gadget lover, and if you're a true gadget lover you are going to trip all over yourself to be the first on your block to get one of these. It looks so great on your scope that it's almost an incidental bonus that it actually does something useful.

"It" is a dial indicator, a machinist's measuring tool that looks like a pocket watch on a pogo stick. Push the stick in and what looks like a minute hand spins around the dial measuring thousandths of an inch, while what looks like a second hand spins around measuring tenths.

How is this useful to an imager? It is useful when you focus. There is a multitude of ways out there to get good focus but *best* focus is a nebulous place that can really be identified only when you've lost it, and that is how this tool works. Find focus and back off to just the point where you are beginning to lose it, then set zero on the dial (the bezel rotates). Now go to the other side of focus, again to the point where you are just beginning to lose it, and note the reading. Best focus is midway between the two.

This gear would once have been beyond the reach of many imagers but the present flood of offshore goods has brought the price down to that of dinner at the pub. Add the magnetic base and arm and it's dinner for two. You will need to make a small right-angle bracket that mounts at the end of the dovetail plate or on the finder bracket or elsewhere on your scope. The arm assembly unscrews from the magnetic base and mounts to your bracket, the dial indicator clamps to the arm, and with a bit of adjustment it's ready to go.

Figure 1 — The dial gauge fitted to a Schmidt-Cassegrain telescope.

It works well...and my but it looks good!

The dial indicator and base come in a set from Lee Valley Tools (www.leevalley.com), Catalog number 88N31.01.

Don Van Akker and his observing partner Elizabeth focus on the stars from Salt Spring Island, B.C. Don will help with this or any other Gizmos project if you email don@knappett.com.

I Can See Clearly Now

by Guy Nason, Toronto Centre (asteroids@toronto.rasc.ca)

I can see clearly now,
The rain has gone.
I can see all obstacles in my way.
Gone are the dark clouds that had me blind...

— Johnny Nash
From the album, *I Can See Clearly Now*
© 1972

On 2008 April 7 (EDT), I observed and recorded the occultation of an 8.7 magnitude star in Cancer (specifically, TYC 1401-00822) by the asteroid (667) Denise (Figure 1). Unlike so many of my previous occultation misadventures, where I set up under clear skies only to be clouded out at the last minute, this time I set up under clouds, but was rewarded when skies cleared with just enough time to find the target star and make the observation.

Figure 1 — The predicted path of Denise across Ontario. Solid lines depict the edges of the predicted occultation path. Dotted lines are the 1-sigma lines.

It was a long night. I left Toronto at 18:00 and arrived at Bruce Peninsula National Park just south of Tobermory (Figure 2) at 21:30. The Clear Sky Chart predicted clouds across my route but left the tip of the Bruce Peninsula clear. What the Chart did not advise me of was the massive electrical storm I encountered just north of Owen Sound. This was one serious — and very unexpected — tempest for this time of year. The rain was torrential and lightning flashes were so nearly constant that my headlights were almost unnecessary. This was more like a midsummer storm than an early spring one.

What to do? Should I give up, cut my losses and turn back, or press on regardless, in hopes I'd run out of storm before I ran out of peninsula? Earlier in the drive north, I had had much time to contemplate the recent jump in fuel prices. Now I seriously began to doubt the wisdom of travelling so far in pursuit of what was clearly a very uncertain enterprise. "Aw, what the heck? Two hours into a three-hour trip is no time to quit," I rationalized. So, regardless, I pressed on.

And what do you know? By the time I arrived at Cypress Lake Campground, 12 km southeast of the predicted path, the rain had stopped and small gaps in the clouds began to appear. When Polaris and a couple of other bright stars peeked out, I quickly aligned the "GoTo" mount and sent it off to find M44 (jumping off point for my star-hop to the target star) even though that part of the sky was still obscured.

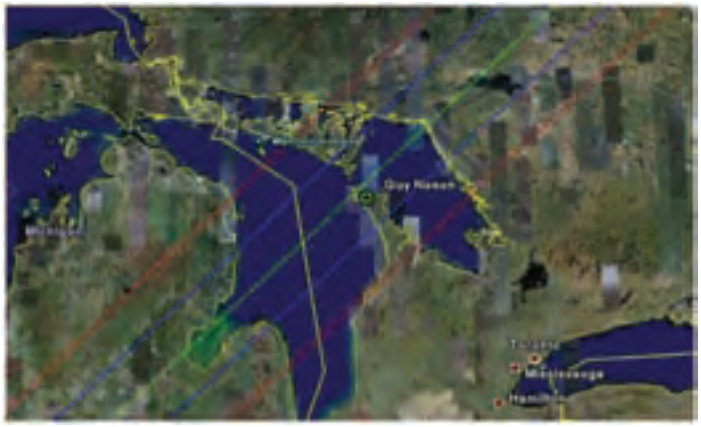

Figure 2 — The path as Google Maps saw it. Green line = predicted path centreline; Blue lines = path edges; Red lines = 1-Sigma lines; Green circle = my location (obviously).

Cancer cleared about five minutes before the predicted occultation time. But because the time was so short between the appearance of the target star from behind the clouds and its disappearance behind the asteroid, I had no time to install the video camera on the telescope or to prepare the rest of the video gear. Instead, I kept it simple (and quick!) by falling back to my trusty short-wave radio and portable tape recorder and observing visually with a low-power eyepiece. In my haste, however, I was not certain that I was "on" the right star — so when it blinked out 14 seconds early, I was doubly surprised and took a bit longer than usual to react and yell "Gone" into the tape recorder. It reappeared after about seven seconds, but I was ready this time and I yelled "Back" with no more than my usual reaction time. After a brief celebration, I packed up all the gear and was on the move again by 23:30, arriving home at 03:15. Time and fuel well spent, as it turned out.

On analyzing the tape and applying my "personal equation" (estimate of my reaction times), I concluded that, from my station, the occultation lasted for 7.5 seconds, from 22:50:38.6 until 22:50:46.1, give or take a few tenths. The predicted maximum duration was 9.3 seconds, which would seem to indicate that the asteroid shadow passed pretty much where it was expected. However, two stations farther "upstream"

in central Texas, occupied by Mike McCants and the duo of Paul Maley and David Weber, recorded longer durations, even though they were even farther SE of the centreline (19 km and 33 km, respectively) than I was. Also in Texas, Richard Nugent observed a miss on the north side and thereby established a loose constraint on that side of the asteroid. Frank Dempsey (Toronto Centre) established an even looser limit to the south side from his Pickering, Ontario, observatory, more than 200 km south of the path, as expected, but his observation could have been useful had the path shifted significantly farther south.

Our preliminary results suggest that the path had shifted by at least 30 kilometres southward and that Denise was approximately 14 seconds "ahead of herself" in her orbit. However our three chords are in good mutual agreement (Figure 3), suggesting a spherical shape to the asteroid — in this profile anyway.

This occultation by (667) Denise was my tenth successfully observed asteroidal occultation, which, as far as I know, is a Canadian record. I hasten to point out, however, that this is a puny accomplishment in light of others' successes. My tenth was also Paul Maley's 88th! Several others in Europe and Japan are well into double digits. And no one knows how many IOTA President David Dunham has observed. He hasn't kept track, but there is no doubt that he has observed, recorded, and reported well over 100 asteroidal occultations. I can see clearly now that I have a long way to go to match these gentlemen!

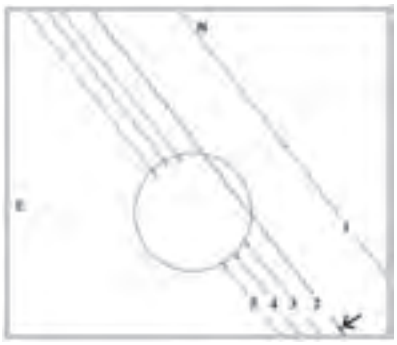

Figure 3: The profile of Denise derived from the set of occultation observations and non-observations. Circle fit based on observations of 2008-04-08 UTC. Chord 1: Richard Nugent, Pontotoc, Texas. Chord 2: predicted orbit of asteroid (667) Denise — the arrow indicates where the centre of the asteroid was expected to be at the time of the occultation. Chord 3: Guy Nason, Tobermory, Ontario. Chord 4: Mike McCants, Kingsland, Texas. Chord 5: Paul Maley and David Weber, Horseshoe Bay, Texas.

Here is a list of possible occultations over populated parts of Canada for the next two months. For more information on events in your area, visit the IOTA Web site, `www.asteroidoccultation.com`. It is very important that you advise me or another IOTA member if you plan to observe and time an event so we can avoid duplicating chords.

DATE(UT) 2008	ASTEROID #	Name	STAR MAG	Δ-MAG	MAX DUR	PATH
Aug. 15	931	Wittemora	11.9	2.2	7.3	nwBC
Aug. 16	28	Bellona	13.3	0.3	15.6	nwON
Aug. 17	804	Hispania	13.5	0.4	10.8	AB, eSK
Aug. 19	5022	1984 HE1	10.1	6.3	4.3	nAB - cBC
Aug. 21	21062	Iasky	9.4	6.5	1.0	Atl. Provs.
Aug. 21	4967	Glia	10.9	4.4	3.2	NL
Aug. 21	27	Eurterpe	11.8	0.6	3.2	wQC - sON
Aug. 24	111	Ate	9.7	2.2	10.8	nMB - sBC
Aug. 28	776	Berbericia	12.9	0.7	5.4	seBC - nMB
Aug. 29	314	Rosalia	12.7	1.4	6.9	cON - neON
Aug. 31	8090	1991 RO23	9.4	6.4	1.6	sNS - sON
Sep. 1	866	Fatme	11.6	2.0	7.6	MB
Sep. 2	533	Sara	10.6	3.7	3.8	MB
Sep. 8	1364	Safara	9.7	6.4	4.2	nON
Sep. 8	27	Euterpe	12.7	0.3	3.6	seQC - cON
Sep. 9	1319	Disa	10.2	6.0	1.5	Atl. Provs.
Sep. 9	687	Tinette	8.7	5.7	3.2	MB
Sep. 11	1337	Gerarda	10.7	5.1	4.2	nwON
Sep. 11	3063	Makhaon	11.8	4.1	7.6	nSK - swBC
Sep. 12	9	Metis	6.0	3.9	48.3	nNL - cON
Sep. 13	914	Palisana	12.1	1.1	35.4	NL
Sep. 13	382	Dodona	11.3	3.9	3.9	NS - NL
Sep. 14	378	Holmia	9.1	4.3	3.0	neMB - swAB
Sep. 14	1240	Centenaria	10.0	4.9	3.3	swAB - nwMB
Sep. 14	542	Susanna	11.3	1.5	3.9	nAB - swBC
Sep. 15	141	Lumen	12.7	0.3	19.5	swNS - swON
Sep. 16	252	Clementina	10.9	2.6	6.2	nQC - cON
Sep. 17	368	Haidea	12.5	3.7	3.0	sBC - nwON
Sep. 18	26984	Fernand-Roland	9.5	6.7	1.3	nAB - sBC
Sep. 18	205	Martha	6.7	6.8	9.7	nwBC
Sep. 18	1356	Nyanza	10.5	5.3	2.4	seSK - nwON
Sep. 19	205	Martha	13.0	1.0	9.9	nwON - seSK
Sep. 20	5022	1984 HE1	9.3	6.7	2.7	seNL
Sep. 21	5372	Bikki	9.6	6.0	1.3	NL - sAB
Sep. 23	2204	Lyyli	11.3	5.4	2.4	sQC - seON
Sep. 23	334	Chicago	12.9	1.1	14.3	nwON - seSK
Sep. 24	859	Bouzareah	12.7	1.5	5.8	nwON
Sep. 25	568	Cheruskia	13.0	0.8	7.9	sBC
Sep. 26	216	Kleopatra	7.7	2.4	15.0	nAB - nBC

Terrestrial Trio

by Bruce McCurdy, Edmonton Centre (bmccurdy@telusplanet.net)

Squint low into the gathering dusk this September, and look for a gathering of a different type. For the first time in a generation, Earth's three terrestrial neighbours will be accessible within the field of view of a standard pair of 10 × 50 binoculars.

Such a cluster of three planets is sometimes incorrectly called a triple conjunction, a term that really means three different conjunctions of the same two planets over a short period of time, generally due to the retrograde motion of one of them. Better to refer to them as a trio or grouping — in the current instance, one that involves three different conjunctions of three different pairs of planets in remarkably short order.

The *Observer's Handbook 2008* (Kelly 2007) neatly summarizes the sequence of events in its Sky Month by Month section:

Thu Sep. 11	4h UT: Mercury at greatest elongation E (27°)
	4h: Mercury 4° S of Venus
	20h: Venus 0.3° N of Mars
Fri Sep. 12	21h: Mercury 3° S of Mars

The first item is important in that Mercury is almost as far removed from the Sun as it can possibly get. Planetary groupings, especially those involving inferior planets, are often a victim of sunblind.

The table on the top of that same Handbook page (112) shows that at 0h UT on the 11th, the three are virtually co-aligned, between 12h52 and 12h54 RA. Not quite perfect, but unusually close. At 11h18m, the Sun is, in theory, over an hour and a half ahead of the threesome. Alas, the next section of the table reveals the unfortunate truth: the relative declinations of the four are truly unfavourable for northern hemisphere observers. The Sun towers 10° in declination higher than Mars and Venus, with Mercury lingering a further 3° even further south.

During autumn evenings, the ecliptic lies at an unfavourably flat angle to the horizon. Solar System objects to the east of the Sun, such as a waxing crescent Moon, reveal the impending path of the Sun as it continues its dive towards the winter solstice point in Sagittarius. This southerly or "horizontal branch" of the ecliptic is the bane of lunar and planetary observers. A lunar observer who has some flexibility of when to observe, will best see a first quarter Moon on a spring evening, or a third quarter phase on an autumn morning, in each case when the advantageous "vertical branch" of the ecliptic is manifest and the Moon is of a high declination relative to the Sun. But in the case of a temporary event such as our terrestrial trio, there is no choice: one simply has to accept the reasons why circumstances aren't as good as they seem to be, find a clear west-southwestern horizon, and get an early start in expectation of a challenging observation. Or fly south, where it is spring and the geometry for evening viewing is favourable.

Alas, any observation involving Mercury and a darkish sky is likely to favour southern hemisphere observers. The aphelion of the innermost planet's highly eccentric orbit is oriented along the southern branch of ecliptic, and the planet's relatively steep inclination further exaggerates the effect. This second effect is why Mercury will be over 3° further south than both Venus and Mars, well below the ecliptic. At the end of the day (so to speak), Mercury sets just half an hour or so after sunset, well before the onset of civil twilight. Its favourable elongation means it is a little further removed from the glare of the Sun, but this is a mixed blessing because Mercury near its aphelion is *literally* further from the Sun, and receiving less than half of the solar intensity it experiences around perihelion, and so is relatively dimmer by close to a full magnitude. On the evening of September 10, the 57% illuminated Mercury will shine at magnitude +0.2.

Fortunately, the guiding beacon that is Venus is nearby. A binocular sweep just above the WSW horizon should locate Venus readily enough. Get a good focus on Venus and anchor it in the upper right of the binocular field; Mercury, a full four magnitudes dimmer, should eventually emerge as a pinprick in the lower left of the field. Mars, a magnitude-and-a-half fainter still, will be much closer to Venus, to the left or lower left depending on the exact time and circumstances of your observation.

Another option is daytime telescopic observation of the trio. With the aid of setting circles or a GOTO telescope, Venus is easy to locate any afternoon when it's sufficiently removed from the Sun. It can also be swept up in a Dobsonian telescope equipped with a decent finder, although folks using this method may want to take the precaution of setting up the scope in the shade, using a strategically situated building or other local obstruction to protect against a painful glimpse of magnified sunlight.

The three will transit the meridian just below the celestial equator around 3 p.m. local daylight time. A planetarium program can help you determine the relative orientation of the three at the time of observation; make a printout if you don't

have your computer on site. Ruddy Mars should be faint but visible, just south of Venus in the same field of view (above in a Dobsonian, below in an SCT or refractor) and perhaps just a little to the left or the right depending on which date you look, as well as the optical path of your telescope. At just 3.8″, Mars appears just 1/3 the apparent diameter of 11.2″ Venus, which is both larger and closer.

A short downward sweep from Venus will be required to locate Mercury, some 3.5° due south. Use low power, and be patient. Mercury will be midway in size between the other two, some 7″ in extent along its long axis. At elongation, it will be near its half-illuminated phase.

If you get more than one chance to attend the family gathering, observe and consider the relative motions. In the extreme foreground is Earth itself, favourably situated at one end of a four-body alignment. Next comes Mercury, closest of the three at about 1.0 A.U., primarily moving towards the Earth as it turns the corner on its elongation and pretty much maintaining its angular distance from the Sun. Venus is on the far side of its orbit at about 1.5 A.U., gradually moving eastward as it slowly gains a presence in the evening sky. At 2.5 A.U. Mars is also on the far side of its orbit, but moving in the opposite direction as it literally fades into the sunset. Of course Venus and Mars are moving 'round the Sun in the same direction in real space, so how come they appear to do the opposite?

The answer is either obscure or obvious, depending on mindset. Despite its reputation as the gravitational centre of the Solar System, the Sun does move against the sky, completing a full "orbit" in exactly one year. As Earth inscribes its own orbital path, the Sun brilliantly reflects our motion. Think of it as the Anti-Earth, exactly 180 degrees out of phase. As such, the Sun is the third fastest "planet" in the Solar System, faster than Mars but slower than Venus. As they pass behind it, the inferior planets overtake the Sun, whereas the outer planets are overtaken.

September's grouping serves as the focal point of an exceptional cluster of conjunctions involving our rocky neighbours. That of Venus and Mercury is the fifth and final encounter between the two in 2008. This is the second such "quintuple conjunction" (QC) of the two planets in just three years, but the last until 2048 (McCurdy 2005; Meeus 2007). QCs involving our two inferior neighbours — no, that's not a slam! — tend to occur in such pairs followed by lengthy intervals, in much the manner as transits of Venus. QCs are of interest to the conjunction junkie because four of the five must occur under (theoretically) favourable circumstances near an aphelic elongation of Mercury. There are pairs of conjunctions to either side of the Sun, bracketing an invisible one near the middle. Between #1-2 and #4-5 the two planets tend to linger together in the sky for quite a few days.

Only two types of QC are possible, involving Mercury with either Venus or Mars. Mercury zigzags back and forth 1.5 times while its partner dawdles through a passage behind the Sun. Because they are closest in angular velocity to the Anti-Earth, only Venus and Mars have long enough synodic periods to hang within Mercury's range for the necessary interval of about 5-7 months.

Both types are relatively rare: a mean rate of about 3 per century involving Venus and about double that with Mars (see Table 1). But in this exceptional case, the two types are piggybacked together. One day after Mercury ends its QC with Venus, it begins a new one with Mars!

Furthermore, the close Venus-Mars conjunction is the first member of a triple conjunction involving those two bodies. Three conjunctions are as good as it gets for these two,

Table 1.

...	...	...	...	...
1361	1376	1393	1408	1423
1438-40	1455	1470-72	1487	1502-04
1517-19	1534	1549-51	1566	1581-83
1596-98	1613-15	1628-30	1645	1660-62
1677	1692-94	1707-09	1724-26	1739-41
1756	1771-73	1786-88	1803-05	1818-20
1835	1850-52	1867	1882-84	1897-99
1914-16	1929-31	1946	1961-63	1976-78
1993-95	**2008**-10	2025-28	2040-42	2057
2072-74	2087-89	2104-07	2119-21	2136
2151-53	2168	2183-86	2198-200	2215-18
2230-32	2247	2262-65	2279	2294-97
2309-11	2326	2341-44	2358	2373-76
2390	2405	2420	2437	2452
...	...	...	...	...

Table 1 — Distribution of quintuple conjunctions in celestial longitude of Mercury and Mars, 1000-3000. Most QCs occur over two calendar years; just the year of the first conjunction is shown.

Like QCs involving Mercury and Venus, there are long "seasons" where QCs are possible, followed by "hibernations," where they are not. One complete season of 113 QCs is represented above, which occurs in just less than11 centuries. Hibernations of about 6 centuries precede and follow this season, thus there are no further QCs during those 2000 years.

When in season, QCs occur singly or in pairs at very regular intervals of 15-17 years, the Mars opposition cycle. Rows are set at an interval of 79 years, in which Mars completes almost exactly 42 revolutions and Mercury 328. Note the slow evolution in each column from single to paired events and back.

The season begins with five single QCs before pairs become possible and eventually commonplace. That beginning in 2008 will be followed by another QC on Mars' next return in 2010. Eventually the series ends as it began, with five single QCs before they become impossible altogether for a time. In fact, the cadence of singles to pairs is almost identical whether the list is read forward or backward, with just one exception.

All data provided courtesy Jean Meeus (private correspondence, 2008), and organized by the author.

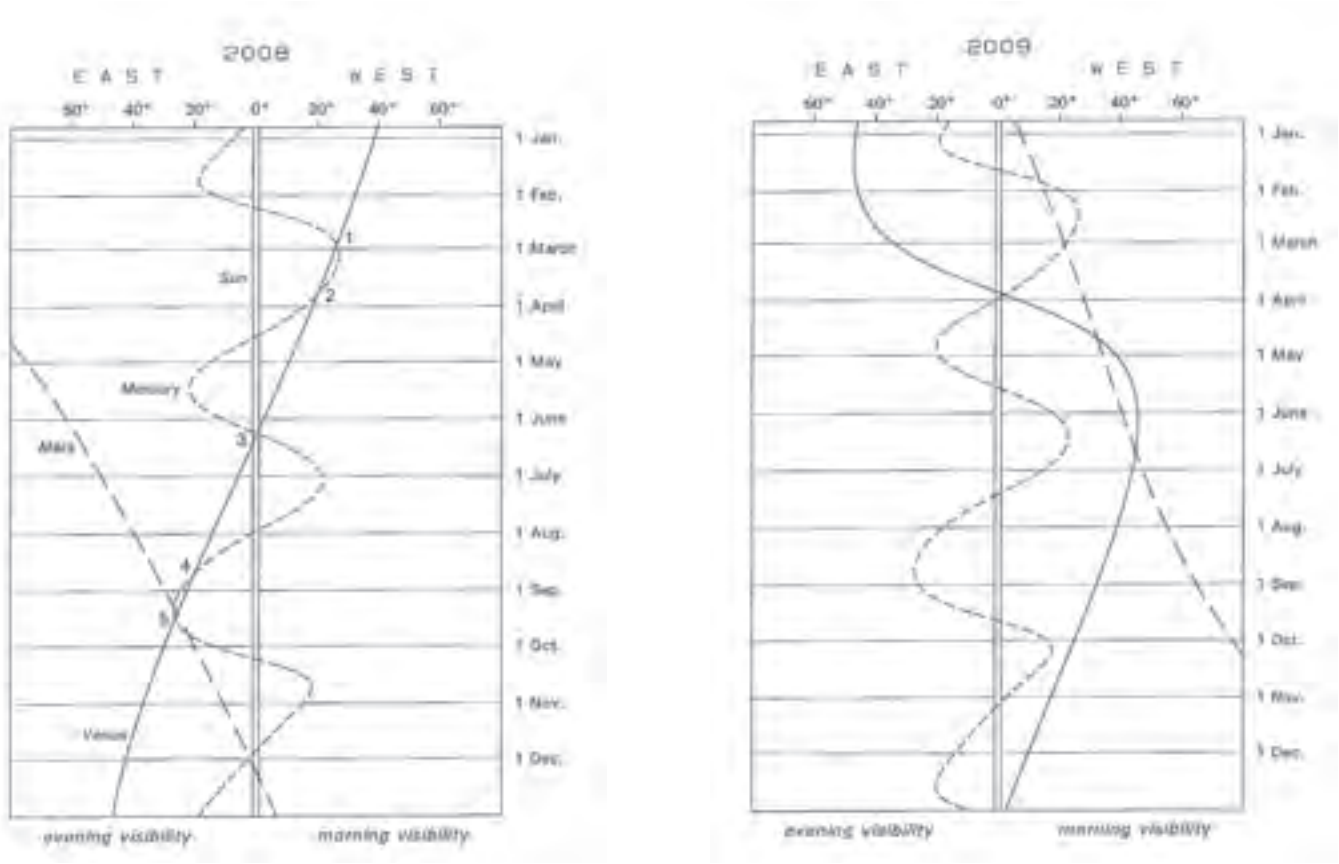

Figure 1 — The relative positions of the Sun, Mercury, Venus, and Mars are shown in these contiguous diagrams for the years 2008 and 2009. The central vertical band represents the disk of the Sun, while the relative positions of the terrestrial planets are given by the three curves. Note how the paths of both Mercury and Venus are much flatter on the left-to-right branch, which represents their passage through inferior conjunction close to Earth. Meanwhile, the curve of Mars becomes more vertical as it passes behind the Sun; its passage through its own perihelion around that time maximizes its velocity and helps it to "keep up" with the Sun for a longer time. QCs with Mercury are only possible around the time of such perihelic solar conjunctions.

In 2008 the path of Venus slices five times through that of Mercury, progressing from right to left (west to east) as it slowly passes through superior conjunction behind the Sun. Mercury meanwhile passes through two such superior (solar) conjunctions and one inferior conjunction, crossing paths with Venus at the points numbered 1 through 5. Paired conjunctions 1-2 and 4-5 all occur near Mercury's maximum elongation and are theoretically observable.

Just as Venus completes the series, Mars enters the grouping from the other side and conjoins with Venus and Mercury in rapid succession, in each case the first conjunction of a series (unnumbered to avoid overcrowding). That with Mercury is a quintuple conjunction, again with four of them favourably placed moderately far from the Sun. This QC takes place a little more rapidly as Mercury undergoes two inferior conjunctions and just one of the superior type. Because Mars is moving in the same direction as Mercury's more rapid motion from evening to morning sky, QCs involving these two planets are slightly more common.

Finally, Mars completes its triple conjunction with Venus with a pair of conjunctions about two months apart at a favourable elongation in the morning sky. Like the other paired conjunctions, note how the two planets will dally fairly close to each other for the entire interval between these last two events.

This figure was graciously provided by RASC Honorary Member Dr. Jean Meeus at the request of the author.

and while such encounters aren't quite so rare, they are still a minority occurrence; of the 47 times Venus overtakes Mars this century, just 17 are triple conjunctions, the rest are singles. Thus there is a full house of conjunctions; 13 in all, involving Earth's neighbours in short order (see Fig. 1). Investigation reveals that at less than 16 months, this is the most compact such grouping in the 2000-year period from 1000-3000. Similar 13-conjunction clusters occur in 1805-06 and 2168-69, at just under 18 months apiece; no other sequence even comes close.

Meeus (1997) provides some further information about how out of the ordinary September's grouping is. In the 71-year period 1980-2050, there are some 40 groupings where three naked-eye planets (Mercury to Saturn, excluding Uranus) are squeezed within a 5° circle. The current instance is unique on the entire table in that it is listed twice: the trio closes within 3°35′ on September 7, then the circle expands slightly before

contracting again to 3°34′ on the 12th. This means this isn't a "one strike and you're out" event; the window of opportunity is about a week.

Only four other times in those seven decades do ME-VE-MA close within a 5° circle, including a morning apparition upcoming on 2011 May 21. Prior to 2008, the two previous groupings occurred far too close to the Sun to be seen. One has to go back to 1976 to find the last observable grouping, when the terrestrial trio closed to within 5° or so in the evening skies of mid-September. That this occurred exactly 32 years ago stands to reason, as the interval represents a near integer number of revolutions for both Mars (17.01) and Venus (52.02). The value for Mercury (100.83) is further from an integer, but near both elongation and aphelion planet's apparent motion is relatively slow, so it would still be in the neighbourhood.

Fast-forward 32 years to September 2040 for an even more interesting situation. Not only will the three rocky planets once again gather east of the Sun, but Jupiter and Saturn will also join the party. The result will be a very rare grouping of all five naked eye planets within 10°, the first visible such quintet since the year 710, with none more until at least 2750. Book your southern vacation now!

References:

Kelly, P., Ed., RASC *Observer's Handbook 2008,* Thistle Printing Limited, Toronto (2007), 112

McCurdy, B., JRASC 99, 72

Meeus, J., *Mathematical Astronomical Morsels,* Willmann-Bell Inc., Richmond, VA (1997), 262

Meeus, J., *Mathematical Astronomy Morsels IV,* Willmann-Bell Inc., Richmond, VA (2007), 277

Bruce McCurdy stayed up all night finishing this column and is too tired to write a bio.

Gerry's Meanderings

The Road Not Taken

by Gerry Smerchanski, Winnipeg Centre (smerch@mts.net)

In a previous article, I investigated how binoculars could be used to observe large-angular-sized objects at low power, but binoculars are not the only tools that can be used to explore this realm. For over a decade, small, economical rich-field telescopes (RFTs) have been available from many sources. These telescopes are designed for low-power wide-field views, but can they replace binoculars? To see if RFTs can be used to the same effect as binoculars, a sampling of such instruments were trained on several of the prime objects that binoculars render well.

Figure 1 — left to right: Generic 8-inch f/4, above it, Stellarvue 80-mm f/6, Sky Watcher 70-mm f/7, Sky-Watcher Equinox 80-mm f/6.25, Accuter Kolibri 750 monocular, and Sky-Watcher 80-mm f/5

The General Comparison

RFTs have one great advantage over most binoculars in that you can easily change magnification by changing eyepieces. This greatly increases the usefulness of these instruments. The other great advantage that RFTs have over most binoculars is that cameras and CCDs can be attached, opening the world of photography to the observer. Imaging is much more awkward with binoculars and in some cases, almost impossible.

The most obvious disadvantage of RFTs is that they usually only allow for viewing with one eye. Yes, binoviewers can be used on these scopes, but for most, this requires the use of a Barlow lens or projection optics to allow the binoviewers to come to focus. The resulting increase in magnification and narrowing of field takes these scopes out of the low-powered realm we wish to explore. Even those RFTs that are modified (tubes shortened) so that binoviewers can be used without additional magnification have to contend with the possibility of vignetting that can occur when eyepieces with a wide field of view are used in a binoviewer that already has a limited clear aperture. Using a binoviewer with RFTs results in a dimmer view in scopes that are already "aperture challenged." However, there can be no general condemnation of binoviewers in these instruments, and for certain optical combinations and targets, the binoviewer can render views as good as or better than a comparable pair of binoculars.

The other aspect that distinguishes RFTs from binoculars is that in most instances the RFTs must be on mounts when

used, though most binoculars, except for the lowest-power versions, also benefit from a secure perch. RFTs can also accommodate right-angle diagonals, making the viewing more comfortable. Many binocular users will attest to the stiff necks they get from extended viewing of high-altitude objects.

Observational Testing

As fortune would have it, Mars was passing through the Beehive (M44) during the test period, providing an excellent background for the evaluation. All of RFTs could frame the Beehive at lowest power, but the view was "tight," and the cluster's nature was somewhat lost. In compensation, the colour and visually pleasing pairings of several of the stars in the cluster were more evident in the higher-powered views. As Mars departed the cluster, the juxtaposition of planet and cluster was lost, limiting the number of nights where the two could be viewed in the same field of view (FOV). The RFTs were essentially limited to a 3° FOV. Low-powered binoculars, with a true FOV twice that of the RFTs, proved to be the better for viewing during the many nights that it took Mars to pass through the cluster.

The same conclusions hold for the other fortunate pairing in the sky those days — Saturn and Regulus. The RFTs never really provided a worthwhile view of these two as a pair though they gave views superior to those of binoculars when each was examined individually. However, the ability to change eyepieces was a big advantage, as even the little 70-mm Sky-Watcher gave respectable views of Saturn and its rings when a 5-mm eyepiece (100×) was inserted. The versatility of these little scopes was a big plus here.

After an eastward sweep across the sky, the next test object was the Coma Berenices star cluster also known as Melotte 111. Over 5° in size, this cluster could not be framed by any but the lowest-power binoculars. The RFTs were consigned to looking at small portions of the cluster, and its nature was lost entirely. The same situation held for views of the asterism and ex-constellation Poniatowski's Bull. It appears as a small "v" asterism to the unaided eye but takes on real character when viewed through binoculars. It was once thought that most of the stars here were members of the loose open cluster Collinder 359, but only 67 Ophiuchi is now regarded as a member. These stars are often used in locating nearby Barnard's star.

The nearby large open cluster IC 4665 can be framed by the RFTs, but, as in the case of the Beehive Cluster, the framing is too tight to reveal the cluster's true nature. Again, low-power binoculars gave the more rewarding view. This distinction was reinforced when I turned to that "odd couple" of open clusters, NGC 6633 and IC 4756. Binoculars framed the pair while the RFTs even had trouble exposing the cluster nature of IC 4765 due to the cluster's large size. The RFTs that could use 2-inch eyepieces did better at encompassing these objects than those restricted to 1.25-inch eyepieces, the 2-inch eyepieces having the widest apparent FOV. However you cut it, low-power binoculars still gave the best views of these stellar assemblies.

The general theme became quite clear — single-tube instruments are no substitute for low-power binoculars for the wide-area objects in the night sky. The RFTs could substitute for higher-powered binoculars, however, if I were willing to give up two-eyed viewing or if imaging were a factor. For purely visual work, the binocular views were still preferred.

The Test Subjects

Sky-Watcher Equinox 80-mm f/6.25 Pro-Series is the flagship of this little fleet. It's a heavy and solid piece with slick features such as a retracting dewshield, two-inch format, and rotating two-speed focuser. Its apochromatic performance gives it a contrast and brightness that the other scopes could not match. This scope also showed the best ability to handle higher magnifications and was the most versatile of the bunch. The drawback is that, at over $600, it costs three times as much as its achromatic sibling described below.

Figure 2 — Sky-Watcher Equinox 80-mm f/6.25 Pro-Series

Stellarvue 80-mm AT1010 f/6 is a popular upscale achromat from a few years ago, now succeeded by the Stellarvue Nighthawk. The former has a sharp, wide FOV that accepts 2-inch accessories. It shows more chromatic aberration and it doesn't have the magnification range of the Equinox 80. When used with a 2-inch diagonal, it has trouble reaching focus with some eyepieces, needing lots of "in" focus. Otherwise, it is a very capable scope.

Sky-Watcher 80-mm f/5 is the scope that had the best potential to substitute for binoculars due to its fast f/ratio. Its one big drawback is that it is confined to 1.25-inch format eyepieces. With a 2-inch focuser this scope would be the thrifty choice as an acceptable substitute for larger binoculars.

Sky-Watcher 70-mm f/7 is a surprising little scope that gave very good images for its size and even acquitted itself adequately when turned to Saturn. The smaller aperture does

not hurt it as much as the f/7 optical configuration, which limits the maximum FOV.

Figure 3 — Sky-Watcher 80-mm f/5.

Figure 4 — Sky-Watcher 70-mm f/7

Accuter Kolibri 750 is a small portable monocular/spotting scope that was the smallest instrument in the test. It doesn't have interchangeable eyepieces and is essentially half of a pair of binoculars. Its advantages are compact size and light weight, which might be a telling factor when hiking. The optics are quite good, though for most astronomical situations a pair of binoculars would be preferred.

Generic/no name 8 inch f/4-4.5 reflectors with their much greater light gathering ability and fast focal ratios should be ideal competitors to the other RFTs tested here. On paper, they fit the bill, with a large true FOV and the potential to use binoviewers without significant significant dimming. Unfortunately, the two examples of this scope that I examined had rather poor optics and were frustrating to use. They required careful collimation (due to the fast focal ratios) but had such poor mechanisms that the collimation was poorly preserved. When they were set up for lowest magnification, the shadow of the large secondary made its presence known. It's a pity that these two examples suffered these quality and design problems, because there is potential for this type of scope to be quite useful for wide-scale viewing. The quality issues during this test may be isolated instances, but a thorough test of these scopes before buying seems prudent.

Conclusion

The small RFTs performed admirably for the most part and fill a definite niche in observing plans. While they might be able to substitute for larger binoculars when observing smaller objects, they do this with the penalty of reverting to single-eyed viewing. For the largest objects in the low-powered observing realm, there still is no substitute for a wide FOV pair of binoculars. If imaging is a goal, then RFTs become the only choice, but when supplemented with low-power/wide FOV binoculars, they can cover the undiscovered country that is missed by larger instruments.

Gerry Smerchanski's interest in astronomy extends at least as far back as his second spoken word, which was "Moon," but it took a leap forward when he obtained his first department store telescope in 1969. Gerry is a scope-aholic and suffers from "ocularosis," which is defined as the inability to ignore eyepieces and other optical equipment.

Help Wanted

Be the First

Want to be the first to get the *Journal?* See the news before anyone else?

The JRASC needs a few more Assistant Editors to read and revise copy before it goes to press. If you have a broad background in astronomy (or have the Web address of Wikipedia memorized), know a good sentence from bad, can organize ideas, enjoy digging to check facts and ideas, and understand how the *Journal's* reference style works, then we can use you on the Production Team.

Duties involve reading copy submitted to you by the Editor and returning it with suggestions and corrections, without submerging the originating author's style in your own. Ability to work quickly — within a week, usually — is essential. Time investment: a couple of hours every two months.

Contact the editor (editor@rasc.ca) for details or to volunteer.

Wanted: Contributing Editors

The Journal is looking for a few good men and women who want to share their expertise with the other RASC members. If you have expertise in the following areas and can write a succinct, insightful column, then we'd like to hear (and read) from you. Here are some bi-monthly columns we'd like to promote:

- Spend too much time playing with computer programs? We want someone to test drive astronomy software. This would be for freeware and shareware only at the start. What freeware? Try *Guidedog, PHD Autoguiding, Carte du Ciel, HNSky,* and on and on. Go exploring and bring it back to the members. Make sure you try it out first.
- Like to find and explore obscure astronomy Web pages? We want someone, or someones, to go digging in the dark recesses of the Web to find resources that will be of value to all levels of amateur astronomy. The more obscure, the better, and it will be up to you to evaluate the site and its treasures. We're not talking *Hubble* here, but stuff like the Bradford Remote Telescope (look it up).
- Are you into the Sun, Moon, and planets? We need a Solar System guru. Must want to delve into the latest professional science and bring back a story we can all follow. Helps if you do your own observing too. In fact, I'd say it's essential. Pretty pictures are nice, but is the latest solar cycle a little late? It's up to you to find out and tell us why. Try interviewing a few experts on-line, or read the latest ApJ.

The real challenge: each bi-monthly contribution should take no more than **one page** - and that includes pictures. Send a sample column to editor@rasc.ca.

Quick Picks for Observing

by Kim Hay, Kingston Centre (cdnspooky@persona.ca)

September 2008	**Event**
Monday Sep. 8 0:12 UT	Double shadow transit on Jupiter
Tuesday Sep. 9 3:00 UT	September Perseid Meteor peak *
Thursday Sep. 11 4:00 UT	Mercury at greatest elongation** **Challenge Observation!!**
Monday Sep. 15 9:13 UT	Full Moon - Harvest Moon
Taken from Norse mythology, this is the Full Moon closest to the autumn equinox. For other names and mythology of Full Moons, see `http://en.wikipedia.org/wiki/Harvest_moon` for more information	
Friday Sep. 19 5:00 UT	Moon 1.0° N of Pleiades (M45)
Monday Sep. 22 15:45 UT	Autumn Equinox
Sunday Sep. 28	Zodiacal Light ***
Sunday Sep. 28 0:00 UT	δ Aurigid Meteor Peak *

October 2008	**Event**
Saturday Oct. 4	**Fall Astronomy Day –** Across the RASC
Fall Astronomy Week 2008 Sep. 29 - Oct. 5. **See** `www.rasc.ca/astroday/resources.shtml` for more information	
Wednesday Oct. 8	Draconid meteor shower * 1:00 UT peak time
Tuesday Oct. 14 20:02 UT	Full Moon - Hunter's Moon see `http://en.wikipedia.org/wiki/Harvest_moon` for more information.
Tuesday Oct. 21 4:00 UT	Orionid meteor peak 20 ZHR*
Wednesday Oct. 22 10:00 UT	Mercury at greatest elongation West (18°) **
Monday Oct. 27	Zodiacal Light ***
Tuesday Oct. 28 23:14 UT	New Moon (lunation 1062) ≈
Basic data on symbols and the Greek alphabet are located on **page 20** of the ***Observer's Handbook***	

November 2008	**Event**
Monday Nov. 3 22:00 UT	Jupiter 1.9° N of Moon
Tuesday Nov. 4 4:00 UT	S. Taurid meteor peak *
Wednesday Nov. 12 4:00 UT	N. Taurid meteor peak *
Wednesday Nov. 12	Venus close to M8, visible after dark.
Monday Nov. 17 10:00 UT	Leonid meteor peak ZHR 15 *
Tuesday Nov. 18 10:00 UT	Moon 1.2° S of Beehive M44 Venus near M22, M28
This is a great time to start your winter Messier Observations. See `www.rasc.ca/messier/index.shtml` to work on your Messier Certificate.	
Sunday Nov. 30	Jupiter 2° N of Venus, visible after dark

Starting in September, the next three months is a great time to view the planets and bright stars as they pass a few degrees from the Moon. Look in the *Observer's Handbook* for various times and dates for planet and bright star groupings on **page 113** for September, **page 115** for October, and **page 117** for November.

*** Meteor Showers** for September, October, and November
Read the following pages in the **RASC *Observer's Handbook:*** for information on meteor showers **page 232-233, page 234** for a calendar of meteor shower dates, and **page 235** for radio detection of meteors (use these links for more information: `www.imo.net/calendar/2008`, `www.skyscan.ca/radio_meteor_detection.htm`)

ZHR — Zenithal Hourly Rate — number of meteors an observer would see if the radiant were directly overhead, sky dark, and limiting magnitude of 6.5+.

**** Elongation**
Elongation is the angular distance between a celestial object and the Sun. For more information see **page 20** of the ***Observer's Handbook.***

*****Zodiacal Light:** Zodiacal Light is visible in N lat. in the east before morning twilight for the next two weeks
Zodiacal Light: Interplanetary dust; see **page 248** in the ***Observer's Handbook*** for more information.

≈ **Lunation:** A cycle of phases in one synodic month, starting and ending with New Moon. For example, Sep. 29 will be the start of lunation 1061.

Society News

by James Edgar, National Secretary (jamesedgar@sasktel.net)

As I write this, our President, Dave Lane, is at an IYA conference in St. Louis, Missouri, with members of the IYA2009 Canadian contingent — Jim Hesser and others have met all week with our counterparts in the USA to discuss IYA initiatives and their implementation. Look for a news item from Kim Hay about recent happenings on the RASC Web site, `www.rasc.ca/news/IYA2009-01.shtml` including the hire of a part-time employee, paid through a donation to CASCA. The RASC is handling payroll and incidentals for **Kim Breland.** If you hear from her, show her your usual welcoming hospitality.

Fundraising for IYA2009 is starting to ramp up, which is mostly Kim Breland's involvement. By now, you may have received a letter from the Executive asking you to consider a donation, one that will help us see our projects through from tiny seedlings to large (and lasting), mighty oaks.

Our National Office is seemingly under attack. We've had to evict our former tenant, and a water leak in the basement has caused no end of damage and extra workload. Fortunately, our faithful Executive Secretary, Bonnie Bird, and her interim replacement, Jo Taylor, were on hand to stem the flow and help clean up the mess. Thanks to all who helped out.

In a few short weeks, we'll be attending the GA in Toronto. It promises to be a momentous time, one in which our Society turns a corner — changing for the future. More on that in the next issue.

I trust you all have a great summer and plenty of clear skies with few mosquitoes!

Glory for Glories Sake

by Rick Stankiewicz, Unattached Member (stankiewiczr@nexicom.net)

Description

A "glory" is the name given to an atmospheric phenomenon in which a circular rainbow is seen at a point directly opposite the Sun, centred on the observer's shadow — or at least where the shadow would be if it were visible. More typically, the shadow is that of an aircraft in which the observer is riding, projected on the clouds below. The glory's ring will be centred at the location in the aircraft shadow where the watcher is sitting.

A glory's rings are delicate with blue on the inside, changing through greens to red and purple outside. Sometimes three or even four rings are visible, appearing and disappearing as the aircraft flies over clouds of varying distance and structure

Cause

The phenomenon is produced by backscattered light reflected from clouds of uniformly sized water droplets. The glory's angular size depends only on the size of the water droplets, with small droplets producing large glories. Colours are caused by the diffraction of the light beam through the droplet while the multiple rings are determined by destructive interference of the various rays as they pass through a myriad of droplets. The glory then is a phenomenon that depends on reflection, diffraction, refraction, and interference — surely unique in the field of atmospheric optics.

Observing Glories

The most common situation in which to see a glory is from an aircraft. Glories are always directly opposite the Sun, centred at the antisolar point, and therefore will appear below the horizon from your window-seat perspective. A glory requires a cloud with water droplets, not ice crystals, and so is usually well below the aircraft where atmospheric temperatures are higher. At one point, before the advent of regular air travel, glories were a rare phenomenon, seen only when the low Sun cast an observer's shadow onto a fog bank or onto a cloud during a mountain climb. Their original name — *Brockenspectre* — derives from the Brocken, a prominent peak in Germany's Harz Mountains, where mountaineers first saw it and the original legends began.

With a little bit of planning on your part and a bit of luck on the atmosphere's part, your odds of seeing a glory on your next flight are pretty good. Here are some tips that I have found to work for me over the years.

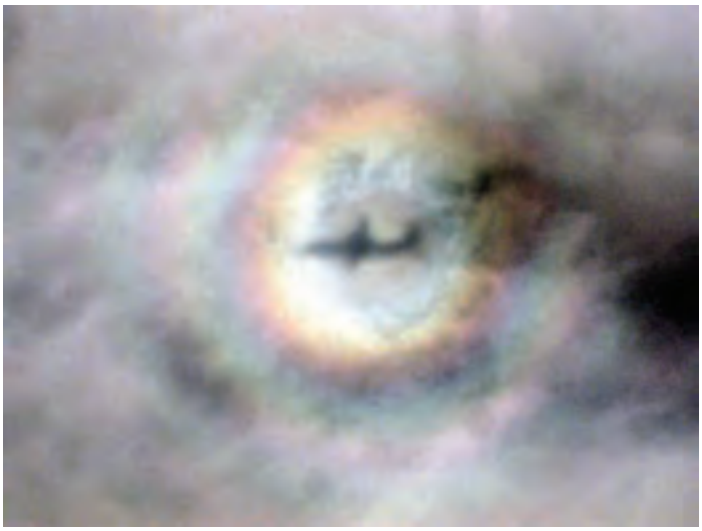

Figure 1 — A glory around shadow of a Dash 8 aircraft *en route* from Toronto to Thunder Bay. Three rings of colour are visible around the aircraft's shadow.

- Consider the direction of your flight path and the angle of the Sun in relation to this path.
- Book a window seat on the side of the plane opposite the Sun. Get a seat assignment that is well forward or well back of the plane to avoid the wing obstruction.
- Flights around mid-day are best, for the Sun will be high, casting a shadow of the plane on the ground within the view from your window seat.
- Have your camera at the ready, keep watching the clouds below and off to the side of the plane. If you see the shadow of the plane, and the right kind of cloud is beneath you, you should easily spot the surrounding rainbow-like ring. With luck, the glory will be bright and have two, three, or even four rings.
- Start taking pictures and good luck. A little underexposure may make the colours stand out better. I used a Nikon 4500 @ ISO 100, f/7.8, 1/575 second to capture the image in Figure 1.

References:

`http://en.wikipedia.org/wiki/Glory_%28optical_phenomenon%29`

`www.atoptics.co.uk/`

`www.philiplaven.com/p2c1a.html`

THE ROYAL ASTRONOMICAL SOCIETY OF CANADA

NATIONAL OFFICERS AND COUNCIL FOR 2008/CONSEIL ET ADMINISTRATEURS NATIONAUX

Honorary President	Robert Garrison, Ph.D., Toronto
President	Dave Lane, Halifax
1st Vice-President	Mary Lou Whitehorne, Halifax
2nd Vice-President	Glenn Hawley, B.Sc., B.Ed., Calgary
Secretary/Recorder	James Edgar, Regina
Treasurer	Mayer Tchelebon, Toronto, MBA, CMA
Past Presidents	Scott Young, B.Sc., Winnipeg and Peter Jedicke, M.A. London
Editor of *Journal*	Jay Anderson, B.Sc., MNRM, Winnipeg
Editor of *Observer's Handbook*	Patrick Kelly, M.Sc., Halifax
Editor of *The Beginner's Observing Guide*	Leo Enright, B.A., Kingston
Editor of *Observer's Calendar*	Dave Lane, Halifax
Interim Executive Secretary	136 Dupont Street, Toronto ON M5R 1V2 Telephone: (416) 924-7973

CENTRE ADDRESSES/ADRESSES DES CENTRES

The most current contact information and Web site addresses for all Centres are available at the Society's Web site: **www.rasc.ca**

Belleville Centre
c/o Greg Lisk, 11 Robert Dr, Trenton ON K8V 6P2

Calgary Centre
c/o Telus World of Science, PO Box 2100 Stn M Location 73, Calgary AB T2P 2M5

Charlottetown Centre
c/o Brian Gorveatt, 316 N Queen Elizabeth Dr, Charlottetown PE C1A 3B5

Edmonton Centre
c/o Telus World of Science, 11211 142 St, Edmonton AB T5M 4A1

Halifax Centre
PO Box 31011, Halifax NS B3K 5T9

Hamilton Centre
576 - Concession 7 E, PO Box 1223, Waterdown ON L0R 2H0

Kingston Centre
PO Box 1793, Kingston ON K7L 5J6

Kitchener-Waterloo Centre
305 - 20 St George St, Kitchener ON N2G 2S7

London Centre
PO Box 842 Stn B, London ON N6A 4Z3

Mississauga Centre
PO Box 98011, 2126 Burnhamthorpe Rd W, Mississauga ON L5L 5V4

Centre francophone de Montréal
C P 206, Station St-Michel, Montréal QC H2A 3L9

Montréal Centre
18455 Meloche St, Pierrefonds QC H9K 1N6

New Brunswick Centre
c/o Paul Gray,1068 Kingsley Rd, Birdton NB E3A 6G4

Niagara Centre
PO Box 4040, St. Catharines ON L2R 7S3

Okanagan Centre
PO Box 20119 TCM, Kelowna BC V1Y 9H2

Ottawa Centre
1363 Woodroffe Ave, PO Box 33012, Ottawa ON K2C 3Y9

Prince George Centre
7365 Tedford Rd, Prince George BC V2N 6S2

Québec Centre
2000 Boul Montmorency, Québec QC G1J 5E7

Regina Centre
PO Box 20014, Regina SK S4P 4J7

St. John's Centre
c/o Randy Dodge, 206 Frecker Dr, St. John's NL A1E 5H9

Sarnia Centre
c/o Paul Bessonette, 160 George St, Sarnia ON N7T 7V4

Saskatoon Centre
PO Box 317 RPO University, Saskatoon SK S7N 4J8

Sunshine Coast Centre
PO Box 577, Sechelt BC V0N 3AO

Thunder Bay Centre
286 Trinity Cres, Thunder Bay ON P7C 5V6

Toronto Centre
c/o Ontario Science Centre, 770 Don Mills Rd, Toronto ON M3C 1T3

Vancouver Centre
1100 Chestnut St, Vancouver BC V6J 3J9

Victoria Centre
3046 Jackson St, Victoria BC V8T 3Z8

Windsor Centre
2831 Alexandra Ave, Windsor ON N9E 2J8

Winnipeg Centre
PO Box 2694, Winnipeg MB R3C 4B3

The CGRT Project

eta Carina — One of the brightest nebulae in the sky, but visible only from the southern hemisphere. Taken by Craig Breckenridge using the Chris Graham Remote Telescope (CGRT).